INFORMATION TO USERS

This manuscript has been reproduced from the microfilm master. UMI films the text directly from the original or copy submitted. Thus, some thesis and dissertation copies are in typewriter face, while others may be from any type of computer printer.

The quality of this reproduction is dependent upon the quality of the copy submitted. Broken or indistinct print, colored or poor quality illustrations and photographs, print bleedthrough, substandard margins, and improper alignment can adversely affect reproduction.

In the unlikely event that the author did not send UMI a complete manuscript and there are missing pages, these will be noted. Also, if unauthorized copyright material had to be removed, a note will indicate the deletion.

Oversize materials (e.g., maps, drawings, charts) are reproduced by sectioning the original, beginning at the upper left-hand corner and continuing from left to right in equal sections with small overlaps. Each original is also photographed in one exposure and is included in reduced form at the back of the book.

Photographs included in the original manuscript have been reproduced xerographically in this copy. Higher quality 6" x 9" black and white photographic prints are available for any photographs or illustrations appearing in this copy for an additional charge. Contact UMI directly to order.

UMI®

Bell & Howell Information and Learning
300 North Zeeb Road, Ann Arbor, MI 48106-1346 USA
800-521-0600

Hydrolytic Cleavage of *p*-Nitrophenyl Esters of N-protected Amino Acids in the presence of Cyclodextrins: Transition State Stabilization

Paul G. Loncke

A Thesis
in
The Department
of
Chemistry and Biochemistry

Presented in Partial Fulfilment of the Requirements
for the Degree of Master of Science at
Concordia University
Montreal, Quebec, Canada

February 1998

© Paul G. Loncke, 1998

National Library of Canada
Acquisitions and Bibliographic Services
395 Wellington Street
Ottawa ON K1A 0N4
Canada

Bibliothèque nationale du Canada
Acquisitions et services bibliographiques
395, rue Wellington
Ottawa ON K1A 0N4
Canada

Your file Votre référence

Our file Notre référence

The author has granted a non-exclusive licence allowing the National Library of Canada to reproduce, loan, distribute or sell copies of this thesis in microform, paper or electronic formats.

L'auteur a accordé une licence non exclusive permettant à la Bibliothèque nationale du Canada de reproduire, prêter, distribuer ou vendre des copies de cette thèse sous la forme de microfiche/film, de reproduction sur papier ou sur format électronique.

The author retains ownership of the copyright in this thesis. Neither the thesis nor substantial extracts from it may be printed or otherwise reproduced without the author's permission.

L'auteur conserve la propriété du droit d'auteur qui protège cette thèse. Ni la thèse ni des extraits substantiels de celle-ci ne doivent être imprimés ou autrement reproduits sans son autorisation.

0-612-39956-7

Canada

ABSTRACT

Hydrolytic Cleavage of *p*-Nitrophenyl Esters of N-protected Amino Acids in the presence of Cyclodextrins: Transition State Stabilization

Paul G. Loncke

The kinetics of cleavage of *p*-nitrophenyl esters of N-*tert*-butyloxycarbonyl amino acids (BOC-Esters) and N-benzyloxycarbonyl amino acids (CBZ-Esters) in basic solution containing α-cyclodextrin, β-cyclodextrin, or γ-cyclodextrin, (α-CD, β-CD, or γ-CD) were studied. Most of the cleavage reactions occur through conventional 1:1 (ester:CD) complexes, and although there are instances where complexation is not evident, reaction may well occur within weak 1:1 (ester:CD) complexes. In some cases, a second cleavage process involving two CD molecules is evident which may be due to reaction between a 1:1 (ester:CD) complex and a second CD molecule, or to reaction within a weak 1:2 (ester:CD) complex. Also, an additional process involving the formation of non-productive 1:2 (ester:CD) complexes is apparent in two cases.

In order to determine the dominant mode of binding for the esters in the 1:1 (ester:CD) complexes, variations in the kinetic parameters with structure were examined, along with circular dichroism studies. Also, based on an approach developed by Kurz,[5,32,33,49] the extent to which the three cyclodextrins stabilize the transition states of the normal ester cleavage reactions was estimated, and used to probe the structures of the transition state complexes.

Cleavage of the *p*-nitrophenyl esters of BOC-Asn, CBZ-Asn, BOC-Gln, and CBZ-Gln in basic aqueous solution involves intramolecular nucleophilic attack by ionized internal amide groups.[59,66] In the presence of CDs, moderate rate enhancements were observed in most cases due to reaction within 1:1 (ester:CD) complexes. However, cleavage of BOC-Asn and CBZ-Asn in the presence of β-CD is initially retarded due to the formation of very stable non-productive 1:1 (ester:CD) complexes, and then enhanced due either to reaction between the non-productive 1:1 complexes and unbound CD molecules, or to reaction within weak productive 1:2 (ester:CD) complexes.

Finally, modest enantioselectivity was observed for cleavage of pairs of *p*-nitrophenyl esters of N-protected amino acid enantiomers in the presence of CDs. For almost every pair of enantiomers, the L-ester is cleaved faster than the D-ester by CDs, even though their cleavage rates in buffer are practically the same. Similar results were seen for cleavage of a pair of N-hydroxysuccinimide esters of BOC-Pro enantiomers. The selectivity observed was shown to be almost entirely due to stronger transition state binding of the L-ester, since both enantiomers bind equally well in the initial state.

Acknowledgements

I would like to thank my research supervisor Dr. Oswald S. Tee for his guidance and patience throughout this project.

I am also very grateful to the following:

- ♥ Dr. Lawrence and Dr. Colebrook for serving on my research committee.
- ♥ Concordia University for financial assistance.
- ♥ My mom, dad, aunts, and other members of my family for their love and support.
- ♥ Dr. Turnbull and Dinesh for help with the circular dichroism spectropolarimeter.
- ♥ Students I have worked with in the past Dr. Tim Gadosy, Mike, Shawn and Chris, and the current members of the lab Alexei, Isabelle, Samer, and Delna.
- ♥ The staff and graduate students in the department of chemistry and biochemistry.

Table of Contents

List of Figures viii

List of Tables xi

List of Schemes xii

List of Abbreviations xiii

1. INTRODUCTION 1

1.1 Brief Overview of Cyclodextrins 1

1.2 Structure, Physical, and Chemical Properties of Cyclodextrins 2

1.3 Cyclodextrin Inclusion Complexes in Aqueous Solution 5

1.3.1 Host-Guest Spatial Fitting 7

1.3.2 Driving Force for Cyclodextrin Complexation 9

1.4 Effects of Cyclodextrins on Reactions 13

1.4.1 Kinetics of Cyclodextrin Mediated Reactions 13

1.4.2 Transition State Stabilization by Cyclodextrins 15

1.4.3 Effects of Cyclodextrins on the Diels-Alder Reaction 18

1.4.4 Effects of Cyclodextrins on Intramolecular Acyl Transfer 19

1.4.5 Effect of Cyclodextrins on the Enolization of 2-Indanone 20

1.4.6 Cleavage of Phenyl Esters by Cyclodextrins 21

2. RESULTS and DISCUSSION 27

2.1 Structure-Reactivity Analysis for Ester Cleavage by α-CD 31

2.2 Structure-Reactivity Analysis for Ester Cleavage by β-CD 39

2.3 Structure-Reactivity Analysis for Ester Cleavage by γ-CD 50

2.4 Effects of cyclodextrins on Intramolecular Ester Cleavage 61

2.5 Enantioselective Cleavage by Cyclodextrins 67

3. CONCLUSIONS 73

4. EXPERIMENTAL 75

4.1 Materials 75

4.2 Kinetic Experiments 75

4.3 Circular Dichroism Experiments 77

References 79

Appendix 84

List of Figures

Figure 1.1 Molecular structure of α-CD 3

Figure 1.2 Overall bucket shape of cyclodextrins 4

Figure 1.3 Converging and diverging binding sites 5

Figure 1.4 Gibbs free energy diagram showing transition state stabilization by CDs 17

Figure 2.1 Structures of amino acid side chains 27

Figure 2.2 Orientations of transition moments of *p*-substituted phenyl derivatives 29

Figure 2.3 Induced c.d. spectra of *p*NPA with α-CD, β-CD, and γ-CD 30

Figure 2.4 Plot of k_{obs} vs $[\alpha\text{-CD}]_o$ for cleavage of BOC-Esters 32

Figure 2.5 Plots of k_{obs} vs $[\alpha\text{-CD}]_o$ for cleavage of CBZ-Esters 32

Figure 2.6 Plot of log k_2 vs log k_u for BOC-Esters with α-CD 35

Figure 2.7 Plot of log k_2 vs log k_u for CBZ-Esters with α-CD 35

Figure 2.8 Induced c.d. spectra of *p*NPA, BOC-Gly, CBZ-Gly, BOC-β-Ala, and CBZ-β-Ala with α-CD 37

Figure 2.9 Effect of α-CD on c.d. spectrum of BOC-L-Ala 37

Figure 2.10 pK_{ts} values for CBZ-Esters vs BOC-Esters with α-CD 38

Figure 2.11 Plots of k_{obs} vs $[\beta\text{-CD}]_o$ for cleavage of BOC-Esters 40

Figure 2.12 Plots of k_{obs} vs $[\beta\text{-CD}]_o$ for cleavage of CBZ-Esters 40

Figure 2.13 Plot of log k_2 vs log k_u for BOC-Esters with β-CD 43

Figure 2.14 Plot of log k_2 vs log k_u for CBZ-Esters with β-CD 43

Figure 2.15 pK_s and pK_{ts} values for BOC-Esters with β-CD 44

Figure 2.16 pK_s and pK_{ts} values for CBZ-Esters with β-CD 44

Figure 2.17 pK_s values for CBZ- vs BOC-α-amino acid esters 45

Figure 2.18 Induced c.d. spectra of BOC-Gly, CBZ-Gly, and *p*NPA with β-CD 45

Figure 2.19 Gibbs free energy diagram showing transition state stabilization by a second CD molecule 47

Figure 2.20 pK'_{ts} values ternary transition state complexes 48

Figure 2.21 Plots of k_{obs} vs $[\gamma\text{-CD}]_o$ for cleavage of BOC-Esters 51

Figure 2.22 Plots of k_{obs} vs $[\gamma\text{-CD}]_o$ for cleavage of CBZ-Esters 52

Figure 2.23 Plots of k_{obs} vs $[\gamma\text{-CD}]_o$ indicating formation of non-productive complexes 52

Figure 2.24 Plot of log k_2 vs log k_u for BOC-Esters with γ-CD 55

Figure 2.25 Plot of log k_2 vs log k_u for CBZ-Esters with γ-CD 55

Figure 2.26 pK_s and pK_{ts} values for BOC-Esters with γ-CD 56

Figure 2.27 pK_s and pK_{ts} values for CBZ-Esters with γ-CD 56

Figure 2.28 Induced c.d. spectra of *p*NPA, BOC-Gly and BOC-β-Ala with γ-CD . . . 58

Figure 2.29 Induced spectra of CBZ-Gly and CBZ-β-Ala with γ-CD 58

Figure 2.30 Effect of γ-CD on the c.d. spectrum of CBZ-L-Ala 59

Figure 2.31 Cleavage of CBZ-Asn methyl ester 62

Figure 2.32 Effects of α-, β-, and γ-CDs on the cleavage of BOC-L-Asn *p*NP ester . 64

Figure 2.33 Effects of α-, β-, and γ-CDs on the cleavage of CBZ-L-Asn *p*NP ester . 65

Figure 2.34 pK_s and pK_{ts} values for L- and D-Esters with α-CD 70

Figure 2.35 pK_s and pK_{ts} values for L- and D-Esters with β-CD 70

Figure 2.36 pK_s and pK_{ts} values for L- and D-Esters with γ-CD 71

Figure 2.37 Plots of k_{obs} vs $[\beta\text{-CD}]_o$ for BOC-Phe enantiomers 71

List of Tables

Table 1.1 Physical properties of the common cyclodextrins 4

Table 1.2 Dissociation constants for inclusion complexes of *p*-nitrophenolate derivatives with α-CD 7

Table 1.3 Effects of cyclodextrins on intramolecular acyl transfer 19

Table 1.4 Parameters for the catalysed enolization of 2-indanone 20

Table 1.5 Kinetic parameters for cleavage of phenyl acetates by α-CD 22

Table 2.1 Constants for cleavage of esters by α-CD 33

Table 2.2 Constants for cleavage of esters by β-CD 41

Table 2.3 Constants for cleavage of esters by γ-CD 53

Table 2.4 Kinetic parameters for intramolecular ester cleavage 63

Table 2.5 Kinetic parameters for D-Esters 68

Table 2.6 Kinetic ratios for L/D enantioselectivity 69

Table A.1 Data for cleavage of BOC-Esters by α-CD 85

Table A.2 Data for cleavage of CBZ-Esters by α-CD 86

Table A.3 Data for cleavage of BOC-Esters by β-CD 87

Table A.4 Data for cleavage of CBZ-Esters by β-CD 88

Table A.5 Data for cleavage of BOC-Esters by γ-CD 89

Table A.6 Data for cleavage of CBZ-Esters by γ-CD 90

Table A.7 Data for cleavage of N-hydroxysuccinimide esters of BOC-Pro enantiomers by CDs 91

List of Schemes

Scheme 1.1 Diels-Alder catalysed by β-CD 18

Scheme 1.2 (a) Mechanism for catalysed enolization by α-CD 21

(b) Mechanism for catalysed enolization by β- and γ-CDs 21

Scheme 1.3 (a) Cleavage of *m*-substituted phenyl acetates by cyclodextrins 23

(b) Cleavage of *p*-substituted phenyl acetates by cyclodextrins 23

List of Abbreviations

CD	Cyclodextrin
c.d.	Circular Dichroism
BOC-Ester	N-*tert*-butyloxycarbonyl amino acid *p*-nitrophenyl ester
CBZ-Ester	N-benzyloxycarbonyl amino acid *p*-nitrophenyl ester
*p*NP	*p*-nitrophenyl
*p*NPA	*p*-nitrophenyl acetate
HSE	N-Hydroxysuccinimide ester
Ar	Aryl or aromatic group

1. INTRODUCTION

1.1 Brief Overview of Cyclodextrins

Cyclodextrins (CDs) are a series of naturally occurring cyclic oligosaccharides made up of D(+)-glucopyranose units.[1-3] These macrocyclic compounds are produced by the action of the enzyme cyclodextrin-glucosyl-transferase on starch which is usually obtained from *Bacillus Macerans*, but can also be acquired from other species of bacteria such as *Klebsiella pneumoniae, Alcalophyl Bacillus* and *Bacillus megatherium.*

The three most common cyclodextrins, α-CD, β-CD, and γ-CD, sometimes referred to as cyclohexaamylose, cycloheptaamylose, and cyclooctaamylose, are made up of 6, 7, and 8 glucopyranose units, respectively. Homologues comprising higher numbers of glucopyranose units (i.e., 9, 10, 11, and 12 for δ-, ε-, ζ-, and η-CDs) also exist.[1,2] However, there are no cyclodextrins with less than 6 glucopyranose units, and conformation-energy map calculations done by Sundararajan and Rao have indicated that this may be due to steric hindrance.[4]

One of the most interesting features of cyclodextrins is their ability to form inclusion complexes with a wide variety of guest molecules.[1-3] This feature, along with their aqueous solubility and non-toxic nature, has made them suitable for use in the food, cosmetic, pharmaceutical, agricultural, and other industries.[2,18] For instance, the stabilization of important ingredients in food products, cosmetics, toiletries, drug formulations, animal feeds, pesticides and so on, as well as the elimination of unpleasant tastes and odours in some food products, orally administered drugs, animal feeds, and related substances, can be achieved by

complexation with cyclodextrins. The bioavailability of essential ingredients in drug preparations, food supplements, animal feeds, and so on, which have poor aqueous solubility, can also be enhanced by complexation with cyclodextrins. Moreover, cyclodextrins are known to catalyse, as well as retard, a number of chemical reactions, exhibiting kinetic features similar to those of enzyme-catalysed reactions such as saturation-type (Michaelis-Menten) kinetics, substrate selectivity, regioselectivity, enantioselectivity, competitive inhibition and other similar features.[1-6] These features make them useful as models for certain enzymes. The features mentioned above are also interesting to chemists since they can be used as a basis for separation techniques, stereoselective synthesis, and much more.

In recent years, there has been tremendous growth in research into other potential applications of cyclodextrins, as well as more efficient ways of producing them. Thus, in the near future, the use of these cyclic oligomers should become common as more is learnt about their capabilities, production technologies improve, and prices drop.

1.2 Structure, Physical, and Chemical Properties of Cyclodextrins

The typical macromolecular structures of cyclodextrins[1-3] are similar to that illustrated in Figure 1.1 for α-CD. As shown in the figure, the glucopyranose units are in a cyclic arrangement and are joined to each other by α-1,4-glycosidic bonds. Each of the glucopyranose units is in a C1 chair conformation which results in an overall shape resembling that of a bottomless "V-shaped" bucket or truncated cone as shown in Figure 1.2. The secondary hydroxyl groups on the C-2 and C-3 atoms of each glucopyranose unit, end up on one side (wider opening) of the bucket, while the primary hydroxyl groups on the C-6

atoms, end up on the other side (narrower opening). Inside the bucket is a ring of glycosidic oxygens between two rings of methine hydrogens. These characteristics result in the exterior of the macromolecule being relatively hydrophilic, while the interior (cavity) is relatively hydrophobic. The cavity has some degree of Lewis base character due to the ring of glycosidic oxygens. Furthermore, there is a ring of intramolecular (inter-glucose) hydrogen

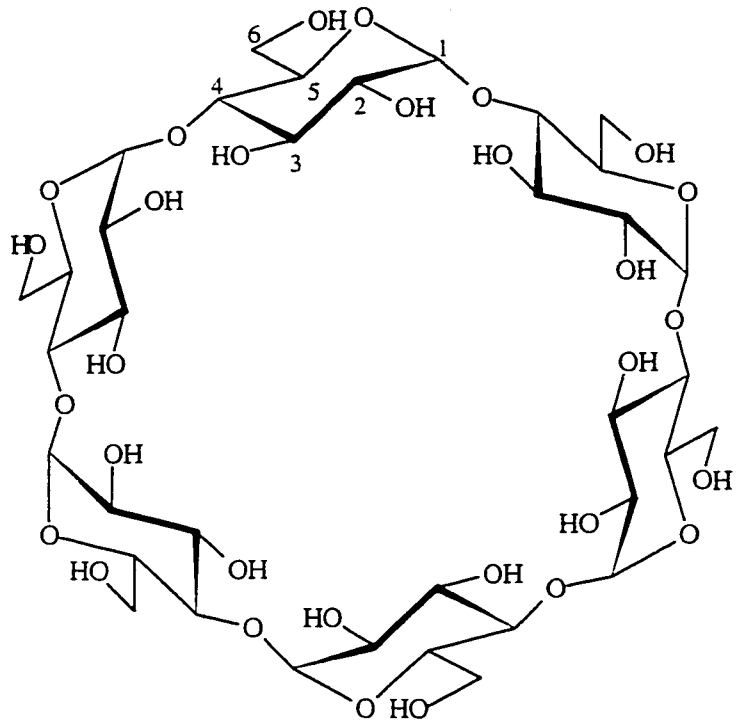

Figure 1.1 Molecular structure of α-CD.

bonds formed between the secondary hydroxyl groups on the C-2 and C-3 atoms of adjacent glucopyranose units which helps to maintain the overall bucket shape of cyclodextrins. This ring of hydrogen bonds also lowers the pK_a of the secondary hydroxyl groups to around 12.3, enhances the aqueous solubility of cyclodextrins, and significantly influences the reactivity of these cyclic oligomers.

Some of the physical properties of the common cyclodextrins are shown in Figure 1.2 and Table 1.1. The cavity depth is essentially the same for all three cyclodextrins, whereas, the cavity width increases from α-CD to β-CD to γ-CD. These compounds have no well defined melting points but usually decompose at temperatures above 200 °C.

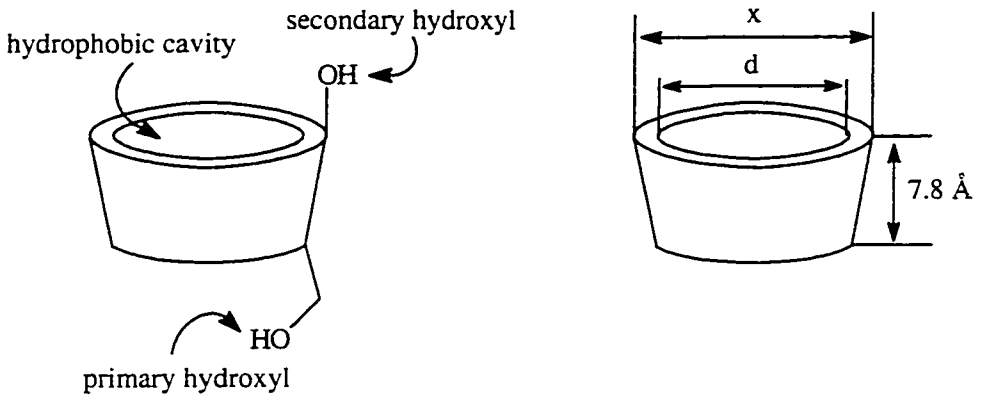

Figure 1.2 Overall bucket shape of cyclodextrins.

Table 1.1 Physical properties of the common cyclodextrins.[a]

Cyclodextrin	n	Molecular Weight	d (Å)	x (Å)	Solubility (g/100 ml H_2O)	$[\alpha]^{25}_D$
α-CD	6	972	5.7	13.7	14.5	150.5 ± 0.5
β-CD	7	1135	7.8	15.3	1.85	162.5 ± 0.5
γ-CD	8	1297	9.5	16.9	23.2	177.4 ± 0.5

[a] From references 1 & 2. n = number of glucopyranose units. $[\alpha]^{25}_D$ = Specific Rotation.

Cyclodextrins have no reducing end groups and thus give positive reactions in tests characteristic of non-reducing carbohydrates.[1,2] They are insensitive to base hydrolysis but do undergo partial hydrolysis in strongly acidic aqueous solution to yield glucose, along with a series of linear maltosaccharides and/or oligosaccharides.[1,2a] In the hydrolysis of acyclic

polysaccharides, the terminal glycosidic bonds are cleaved much faster than their non-terminal counterparts.[2a] Acid hydrolysis of cyclodextrins is initially very slow and this phenomenon has been attributed to the fact that they have no terminal glycosidic bonds.

1.3 Cyclodextrin Inclusion Complexes in Aqueous Solution

Inclusion complexes are macromolecular species in which one molecule (guest) is spatially enclosed in the cavity of another molecule (host).[2a,b] The enclosed guest may cause a slight deformation of the host, but it does not significantly affect the framework of the host, and so the shape and size of the host cavity remains virtually unaltered. The host-guest association involves only non-covalent interactions; no covalent bonds exist between host and

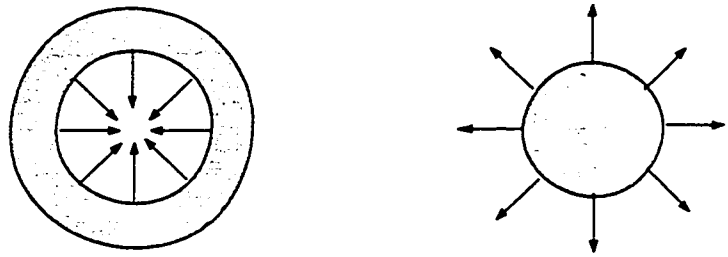

Figure 1.3 Converging and diverging binding sites

guest. One important criterion that must be satisfied for the host-guest association to occur is that the binding sites of the host and guest complement each other stereoelectronically.[2] It is characteristic for the host to have converging binding sites while the guest must have diverging binding sites (Figure 1.3).

In aqueous solution, cyclodextrins are able to spontaneously encapsulate a variety of apolar guest molecules in their cavities. The resulting host-guest complexes are surrounded

by solvate shells of water molecules, and the enclosed guests are oriented so as to maximize contact between their hydrophobic moieties and the apolar cyclodextrin cavities, while their hydrophilic portions remain as much as possible in contact with the aqueous medium. Host to guest stoichiometric ratios of 1:1 are common,[1-3,7,13] but there have been reports of 2:1,[8-12,24] and 1:2 binding,[14] as well as 1:1:1 binding between a cyclodextrin and two different guests.[5,20] These host-guest complexes are not static species but exist in dynamic equilibrium where rapid exchanges between free and bound guest molecules normally occur.[2a,b] Dissociation constants, K_s, are used as a measure of the stability of these complexes, (1.1) and (1.2), from which the Gibbs energy change, $\Delta G°_s$, can be calculated (1.3).

$$S + CD \underset{K_s}{\rightleftharpoons} S.CD \qquad (1.1)$$

$$K_s = \frac{[S][CD]}{[S.CD]} \qquad (1.2)$$

$$\Delta G°_s = -2.303\ RT\ \log K_s = 2.303\ RT\ pK_s \qquad (1.3)$$

The trends in K_s with systematic variations in guest structure can often be used to determine the molecular orientation of a guest inside a cyclodextrin cavity.[1-3,5] For example, ^{1}H-NMR, ^{13}C-NMR, and nuclear Overhauser experiments had previously indicated that the *p*-nitrophenolate anion binds to α-CD with its nitro group first.[15,16] In a subsequent study,[17] methyl substituents were introduced at various positions on the *p*-nitrophenyl ring and the effect on K_s monitored. As shown in Table 1.2, substitution of methyl groups at the 2 and 6 positions slightly weakens binding by a factor of about 2, whereas, substitution of a single methyl group at the 3 position significantly weakens binding by a factor greater than 100.

With methyl substituents at the 3 and 5 positions, no detectable binding occurs. Thus, from the changes in K_s with structure, it is evident that the *p*-nitrophenolate ion binds to α-CD with its nitro group first. In a similar study,[24] variations in K_s with structure indicated that anilinonaphthalenesulfonate isomers bind to β-CD via their naphthyl moieties.

Table 1.2 Dissociation constants for inclusion complexes of *p*-nitrophenolate derivatives with α-CD.[a]

Guest	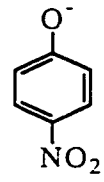	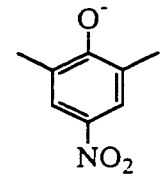	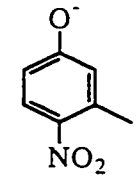	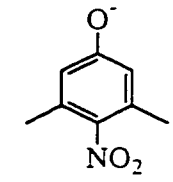
K_S (mM)	0.400	0.942	42.0	No binding

[a] From reference17.

Many techniques have been used to detect and study cyclodextrin host-guest complex formation, - the most widely used being absorption spectroscopy.[1] Other methods include calorimetry, circular dichroism, optical rotary dispersion, fluorescence, NMR, and solubility.[1-3]

1.3.1 Host-Guest Spatial Fitting

The most significant factor influencing the stability of cyclodextrin complexes is the host-guest size compatibility.[1,2,18,19] If the guest is too large, it will not fit into the cyclodextrin cavity and hence no complexation will take place, and conversely, if the guest is too small, it will bind weakly or not at all. Complexation with guests larger than the cyclodextrin cavity may be possible if they contain groups or side chains that can penetrate the cavity or hydrogen

bond to hydroxyl groups on the exterior of the cyclodextrin.

The significance of host-guest size compatibility can be seen by comparing the binding of small guests such as dichloromethane, trichloromethane, and tetrachloromethane,[13] with the larger polynuclear aromatic guests (**1-5**),[8,9,12] to CDs. Dichloromethane is so small that it only binds to α-CD, while the larger trichloromethane, and even larger tetrachloromethane, bind to α-CD and β-CD. However, these three guests are too small to form strong complexes with

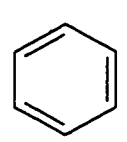

1

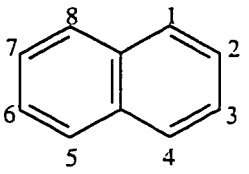

2

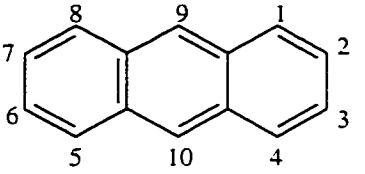

3

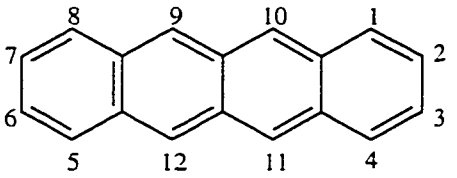

4

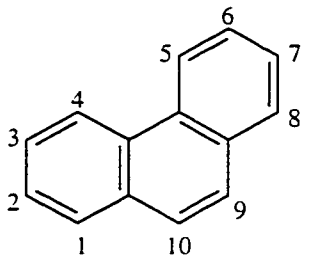

5

γ-CD.[12] In contrast, large guests such as benzene **1**, naphthalene **2**, anthracene **3**, naphthacene **4**, and phenanthrene **5** form fairly stable complexes with γ-CD. Generally speaking, the binding of these polynuclear aromatic guests is strongest to β-CD because they fit snugly into the β-CD cavity in their axial orientations, while they associate weakest with α-CD.

The shape of the guest also plays an important role in the complexation process. For example, *para*-substituted phenyl derivatives such as phenols,[21] phenyl acetates[1] and xylenes,[9] generally form more stable complexes with α-CD and β-CD than their *meta*-substituted counterparts. The stronger binding arises because substituents in the *para* position allow

deeper penetration into the CD, and thus, greater van der Waals interaction with the cavity walls than those in the *meta* position, which tend to hinder binding. Similarly, 2-naphthalene derivatives such as 2-naphthalene sulfonates,[14] 2-naphthyl acetates,[23] and 2-methyl naphthalene,[8] bind more strongly to β-CD and γ-CD than their 1-naphthyl analogues, while anthracene binds more strongly to β-CD and γ-CD than phenanthrene,[12] and 2-anilino-naphthalene-6-sulfonate forms more stable complexes with β-CD than any of its isomers.[24]

1.3.2 Driving Force for Cyclodextrin Complexation

The driving force for cyclodextrin complexation in aqueous solution is likely due to several intermolecular interactions acting simultaneously, resulting in a net decrease in the overall free energy of the system. The extent to which each of these interactions contributes to the driving force depends on the guest and the cyclodextrin. Some of the intermolecular interactions which have been proposed are the extrusion of enthalpy rich water molecules from the cyclodextrin cavity, the relief of cyclodextrin ring strain energy, van der Waals interactions, and hydrogen bonding.[1,2,19,21]

In aqueous solution, water molecules enclosed inside the apolar cyclodextrin cavity (and to a lesser extent those surrounding the apolar guest), cannot satisfy their full complement of tetrahedral hydrogen bonds as well as can those in the bulk aqueous medium and therefore, they are enthalpy rich.[1,2,19,21] Further, these water molecules exist in highly ordered clusters. Extrusion of these high enthalpy water molecules from the cavity upon inclusion of the apolar guest, results in an increase in the amount of favourable interactions (i.e., apolar-apolar interactions between the cyclodextrin cavity and the guest, and polar-polar

interactions between the liberated water molecules and those in the bulk aqueous medium), as well as an increase in the degree of disorder of the system. Consequently, the process should be accompanied by a favourable (negative) enthalpy change, and a favourable (positive) entropy change. Most of thermodynamic data available on cyclodextrin complexation indicate that the process is indeed accompanied by large favourable enthalpy changes, but only small positive or negative entropy changes are observed.[1,14,19,24,25,30]

The number of water molecules that can be accommodated by cyclodextrins increases with cavity size (i.e., α-CD < β-CD < γ-CD). However, as the number of water molecules increases, so does the possibility of them acquiring their full complement of hydrogen bonds, and thus, the less enthalpy rich they become. Therefore, if a guest penetrates the cavities of α-CD, β-CD, and γ-CD to the same extent, resulting in the extrusion of the same number of water molecules, it would form the most stable complex with α-CD. In a similar manner, larger guests which displace more enthalpy rich water molecules than smaller ones, form more stable complexes with cyclodextrins. The fact that naphthacene (**4**) forms more stable complexes with β-CD and γ-CD than benzene (**1**), is consistent with the larger guest being able to displace more enthalpy rich water molecules.[12] Similarly, cyclooctane binds more strongly to β-CD and γ-CD than cyclopentane,[11] while 2-hexanone binds stronger than acetone to α-CD and β-CD.[28]

The macrocyclic conformation of the cyclodextrin in the crystal structure of hydrated α-CD is unsymmetrically distorted, according to x-ray crystallographic studies.[26] However, the conformations are more symmetric in the crystal structures of iodine, 1-propanol, methanol, and potassium acetate complexes. Potential energy calculations indicate that the

conformation of the cyclodextrin in hydrated α-CD is of higher energy than the conformations in those complexes. Based on the assumption that the conformation in the crystal structure is similar to that in solution, it was suggested that strain energy is associated with the hydrated α-CD, which is alleviated upon complexation of a less polar guest. Further, the more symmetric conformation attained by the cyclodextrin upon inclusion of guests other than water, allows the formation of more intramolecular hydrogen bonds between the secondary hydroxyl groups of contiguous glucopyranose units, which contribute in favour of the complexation process.[1-3,26] In hydrated α-CD, only one such bond exists.[26] The relief of ring strain energy may only be significant in α-CD since the conformations of the cyclodextrin rings in hydrated β-CD,[56] and γ-CD,[57] are symmetric. Thus, one would expect larger guests of appropriate size to form more stable complexes with α-CD than smaller guests, since more ring strain energy would be released.

Van der Waals forces generally comprise dipole-dipole interactions, and London dispersion forces. The strength of these interactions increases as the intermolecular distance between two molecular species narrows, and the sizes and polarizabilities of the two species increase. The bulky guest 3,3-dimethyl-2-butanone, $CH_3COC(CH_3)_3$, binds to β-CD about 16 times stronger than its linear counterpart, 2-hexanone.[28] Likewise, *tert*-butanol binds about 3 times stronger than 1-butanol to β-CD.[27] These observations are consistent with stronger van der Waals interactions between the bulkier guest and the cyclodextrin. The stability, expressed as log $(1/K_s)$, of cyclodextrin complexes increases linearly with several physical characteristics of the guest such as alkyl chain length,[21,22,27,29,40-43] total surface area,[10,11,12] molar volume,[11,12] $\log(K_{o/w})$, where $K_{o/w}$ = partition coefficient between organic solvent/water,[21,22,31]

Hammett substituent constant,[1] and so on, which are consistent with increases in van der Waals interactions. These facts seem to indicate that van der Waals forces play a major role in the stability of cyclodextrin complexes.

There is evidence for the existence of hydrogen bonding between 1-adamantane carboxylate and α-CD, but not β-CD.[30] The presence of hydrogen bonding between β-CD and guests such as phenol,[50,51] *p*-hydroxyphenol,[50,51,58] 3-phenyl propionate, 3-(4-hydroxyphenyl) propionate, and 3-(2-hydroxyphenyl) propionate[25] has also been established. However, hydrogen bonding does not always lead to a net stabilizing effect. Thermodynamic studies have shown that hydrogen bonding between β-CD and guests such as 3-(2-hydroxyphenyl) propionate,[25] and *p*-hydroxyphenol,[58] weakens binding relative to the parent compounds because of enhanced unfavourable (negative) entropic contributions. It has also been shown that increasing the hydrogen bond acceptor basicity of several guests leads to a destabilization of the complexes formed with β-CD because of stronger hydrogen bond interactions with water in the aqueous medium.[31] Thus, from the evidence presented, along with the fact that guests which are incapable of being involved in hydrogen bonding form stable complexes with cyclodextrins, shows that hydrogen bonding is not generally important for complexation and may simply occur whenever it is geometrically convenient.

In summary, the driving force for cyclodextrin complexation seems to be due primarily to the extrusion of enthalpy rich water molecules from the cyclodextrin cavity, and van der Waals interaction. The relief of ring strain energy and hydrogen bonding seem to be of lesser importance.

1.4 Effects of Cyclodextrins on Reactions

Cyclodextrins catalysed and retard a number of chemical reactions in aqueous solution via non-covalent and covalent interactions (i.e., non-covalent and covalent catalysis).[1,2,5] Non-covalent catalysis is where the cyclodextrin exerts its catalytic effect by providing an apolar environment (microsolvent effect) or sterically restricted environment (conformational effect) for the reaction. Covalent catalysis arises from the establishment of a covalent bond between the cyclodextrin and the substrate.

1.4.1 Kinetics of Cyclodextrin Mediated Reactions

Consider a substrate, S, which reacts spontaneously in a given medium (1.4), and through a 1:1 (substrate:CD) complex, S.CD, (1.5), to give products, P. The observed rate constant, k_{obs}, should vary with the initial cyclodextrin concentration, $[CD]_o$, according to (1.6) which corresponds to saturation kinetics.[a] In equation (1.6), k_u is the rate constant for the uncatalyzed reaction, K_s is the dissociation constant of the S.CD complex, and k_c is the limiting rate constant at saturating concentrations of cyclodextrin.[1,2a,5,6] Examples of the use of equation (1.6) are given later.

$$S \xrightarrow{k_u} P \qquad (1.4)$$

$$S + CD \underset{K_s}{\rightleftharpoons} S.CD \xrightarrow{k_c} P \qquad (1.5)$$

$$k_{obs} = \frac{k_u K_s + k_c [CD]_o}{K_s + [CD]_o} \qquad (1.6)$$

[a] Assuming $[CD]_o >> [S.CD] < [S]$.

The value for k_u can be measured directly in the absence of cyclodextrin, while values for k_c and K_s can be determined using a non-linear fitting program.[5] Values for k_c and K_s can also be obtained graphically using the Lineweaver-Burk method where $1/(k_{obs} - k_u)$ is plotted against $1/[CD]_o$.[1,2] This plot gives a straight line with a slope equal to $K_s/(k_c - k_u)$ and an intercept equal to $1/(k_c - k_u)$. Another method of obtaining values for k_c and K_s is the Eadie-Hofstee approach where $(k_{obs} - k_u)$ is plotted against $(k_{obs} - k_u)/[CD]_o$, and this gives the slope as K_s and the intercept as $(k_c - k_u)$.

The effects of cyclodextrins on reactions are traditionally examined in terms of k_c/k_u, K_s, and sometimes k_c/K_s.[1] The term k_c/k_u is the factor by which the uncatalyzed reaction is accelerated by saturating levels of the cyclodextrin, while K_s simply reflects the stability of the substrate/CD complex. The apparent second-order rate constant, k_2 (= k_c/K_s), for the reaction of the substrate with the cyclodextrin (1.7), is a measure of the overall efficiency of

$$S + CD \xrightarrow{k_2} P \qquad (1.7)$$

the CD at non-saturating concentrations.[5,6] In cases where the substrate binding appears to be very weak, (i.e., $K_s >> [CD]_o$), k_2 can be obtained from the slope of a plot of k_{obs} versus $[CD]_o$. The terms k_u, k_c, and k_2, frequently vary with the pH of the medium, whereas the term K_s does not, provided that there is no significant protonation or deprotonation of the substrate or the cyclodextrin. Therefore, the terms k_c/k_u and k_2/k_u are more useful for comparative purposes since they are independent of pH. Variations in these two ratios with structure, can provide insight into the mode of transition state binding.

1.4.2 Transition State Stabilization by Cyclodextrins

Catalysis by enzymes and other catalytic agents is believed to arise from the selective binding, and consequent stabilization of the transition state of a reaction.[5,6,32-34,46] Kurz developed a method,[32,33] based on the Transition State Theory,[34,35] for estimating the extent to which a catalyst stabilizes the transition state of a reaction, using experimental data. Tee later used this approach to estimate the transition state stabilization energies of reactions mediated by cyclodextrins[5,49] and other catalysts.[5] Estimation of the transition state stabilization provided by cyclodextrins to the transition states of reactions is as follows.[49]

According to simple Transition State Theory,[35] the rate constants k_u for the uncatalysed reaction (1.4), and k_2 for the catalysed process (1.7), are given by equations (1.8) and (1.9) respectively, where the term ν (= $k_B T/h$) is the frequency with which the transition state decomposes to products. As a starting point, the transition state, TS, for the uncatalysed reaction, is assumed to be the same as that bound to the cyclodextrin, TS.CD, for the catalysed process, which simplifies mathematical and theoretical considerations. It is also assumed that

$$k_u = \nu[TS]/[S] \qquad (1.8)$$

$$k_2 = \nu[TS.CD]/[S][CD] \qquad (1.9)$$

$$K_{ts} = k_u/k_2 = [TS][CD]/[TS.CD] = k_u K_s/k_c \qquad (1.10)$$

$$TS.CD \overset{K_{ts}}{\rightleftharpoons} TS + CD \qquad (1.11)$$

$$k_c/k_u = K_s/K_{ts} \qquad (1.12)$$

ν is the same for the uncatalysed and catalysed processes, and that the transmission coefficients are equal. Once these assumptions have been made, division of (1.8) by (1.9) gives (1.10) which defines a pseudo equilibrium constant, K_{ts}, for dissociation of TS.CD into TS and CD (1.11).[5,49]

The constant K_{ts} is not a true equilibrium constant since it is virtually impossible for the TS.CD complex to dissociate into TS and CD in a reversible manner. However, it does provide information about the relative Gibbs free energy difference, ($\Delta G^{\circ}_{ts} = 2.303\ RT\ pK_{ts}$), between the transition states of the normal and catalysed reactions under standard conditions. Since the derivation of K_{ts} is not based on any particular reaction mechanism, one can use its variations with structure to make reasonable conjectures about the transition state structure of the cyclodextrin catalysed reaction.

The relative Gibbs energies of the various species involved in the uncatalysed and cyclodextrin catalysed reactions are shown in Figure 1.4. The figure clearly illustrates that the transition states of the uncatalysed and catalysed processes are linked by the measurable quantities k_u, k_c, and K_s, and therefore, these quantities can be use to calculate the pseudo equilibrium constant K_{ts}. It can also be seen from the figure that the apparent second-order rate constant, k_2, joins the quantities K_s and k_c. Hence, once K_s and k_c have been determined experimentally, they can be used to calculate k_2.

The Gibbs free diagram shown in Figure 1.4 represents a reaction which is catalysed by a cyclodextrin. It can be seen that the cyclodextrin lowers the free energy of the transition state via complexation which results in a rate enhancement. However, if the substrate forms a very stable complex with the cyclodextrin, the reaction may be retarded or inhibited, since

the energy required to overcome the transition state barrier for the cyclodextrin mediated reaction (i.e., k_c process in Figure 4) may become larger than that required to surmount the transition state barrier for the normal reaction (i.e., k_u process). This can also be seen in (1.12) which implies that the acceleration (or retardation) due to a cyclodextrin, k_c/k_u, depends on the strength of binding in the initial state relative to the transition state. Thus, catalysis arises when the cyclodextrin binds the transition state more tightly than the substrate whereas the reverse is true for retardation or inhibition.

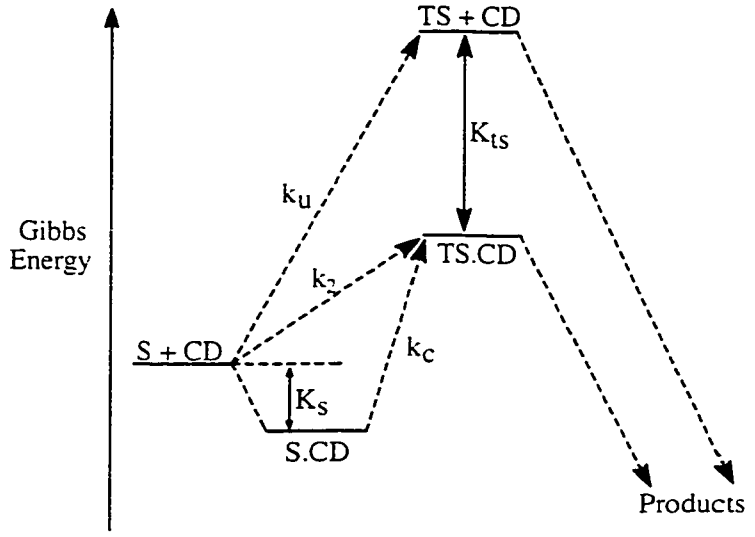

Figure 1.4 Gibbs free energy diagram showing transition state stabilization by CDs.

1.4.3 Effects of Cyclodextrins on the Diels-Alder Reaction

Cyclodextrins exert their "catalytic" influence on the Diels-Alder reaction of cyclopentadiene with acrylonitrile via a microsolvent effect.[20,36] The reaction is accelerated by a factor of 9 when 10 mM β-CD is added to water while a 20% reduction in the reaction rate is observed with α-CD. In the case of β-CD, catalysis is believed to involve a process where both reactants are included in the cavity simultaneously as illustrated in Scheme 1.1.

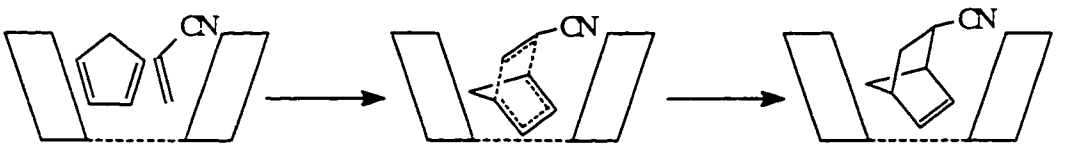

Scheme 1.1 Diels-Alder reaction catalysed by β-CD

There is first an initial association of cyclopentadiene with β-CD, followed by acrylonitrile, resulting in a ternary complex within which the Diels-Alder reaction occurs. The initial binding of the larger and more hydrophobic cyclopentadiene has the effect of increasing the hydrophobicity of the cavity, as well as creating a "smaller cavity" which provides a snug fit for acrylonitrile (i.e., cooperative binding). Simultaneous inclusion of the two reactants in the β-CD cavity has the effect of increasing their available concentrations which favours catalysis. Initial binding of acrylonitrile to β-CD is possible, but the reverse situation is more favourable because of a tighter fit and greater hydrophobic interaction. The α-CD cavity is too small to accommodate both reactants simultaneously and binding of the individual reactants tends to hinder their interaction with each other, thus resulting in retardation.

1.4.4 Effects of Cyclodextrins on Intramolecular Acyl Transfer

The intramolecular transesterification of 2-hydroxymethyl-4-nitrophenyl trimethylacetate, **6**, is accelerated 7-fold by α-CD, but slowed down by a factor of 5 in the presence of β-CD.[1,5,37] The effects of cyclodextrins on the reaction is exerted through a conformational effect. The difference in behaviour between the two cyclodextrins is due to the difference in the strength of substrate binding, since the strength of transition state binding is essentially the same (Table 1.3).[5] In the case of α-CD, the binding of **6** probably favours **6b** which results in a rate enhancement. However, **6** binds very strongly to β-CD and is probably held largely in the unreactive conformation **6a** which impedes the reaction.

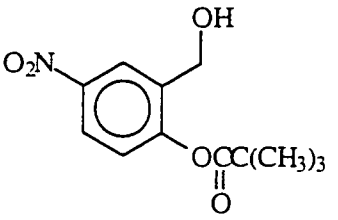

6a

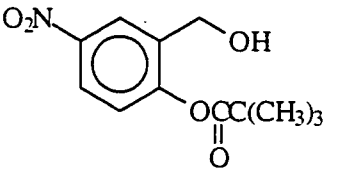

6b

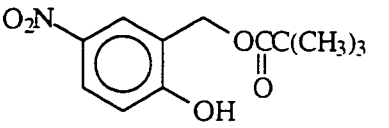

7

Table 1.3 Effects of cyclodextrins on intramolecular acyl transfer.[a]

Cyclodextrin	k_c/k_u	K_s (mM)	K_{ts} (mM)
α-CD	7.33	47.8	6.52
β-CD	0.188	0.960	5.11

[a] From reference 5 & 37.

1.4.5 Effect of Cyclodextrins on the Enolization of 2-Indanone

The enolization of 2-indanone in basic solution is modestly accelerated by α-, β-, and γ-CDs.[38] The catalytic activity is established through covalent interaction between one of the enolizable protons on the substrate and an ionized secondary hydroxyl group on the cyclodextrins. The largest rate enhancement, k_c/k_u, is achieved with α-CD (Table 1.4) which is due to the large difference between the strengths of substrate and transition state binding, while smaller accelerations are obtained with β-CD and γ-CD.

Table 1.4. Parameters for the catalysed enolization of 2-indanone by cyclodextrins.[a]

Cyclodextrin	k_u (s^{-1})	k_c (s^{-1})	k_c/k_u	K_s (mM)	k_2 ($M^{-1}s^{-1}$)	K_{ts} (mM)
α-CD	11.9	262	22.0	59.5	4400	2.7
β-CD	11.7	57.9	4.95	6.49	8900	1.3
γ-CD	11.8	98.2	8.32	60.5	1600	7.3

[a] From reference 38. [b] Done at 25 °C in phosphate buffer, pH 11.6.

The catalysed enolization is believed to proceed as depicted in Scheme 1.2. In the case of α-CD (Scheme 1.2a), the 2-indanone substrate is too bulky to penetrate deep into the cyclodextrin cavity and therefore exists predominantly in the tilted conformation which places the enolizable protons in close proximity to the secondary hydroxyl groups on the CD, thus favouring catalysis. In the cases of β-CD and γ-CD (Scheme 1.2b), the 2-indanone guest is buried deeper inside the cavities of the two CDs which makes the enolizable protons less accessible to the secondary hydroxyl groups, thus detracting from catalysis.

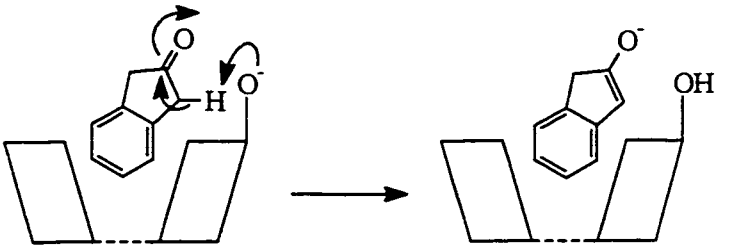

Scheme 1.2a Mechanism for catalysed enolization by α-CD.

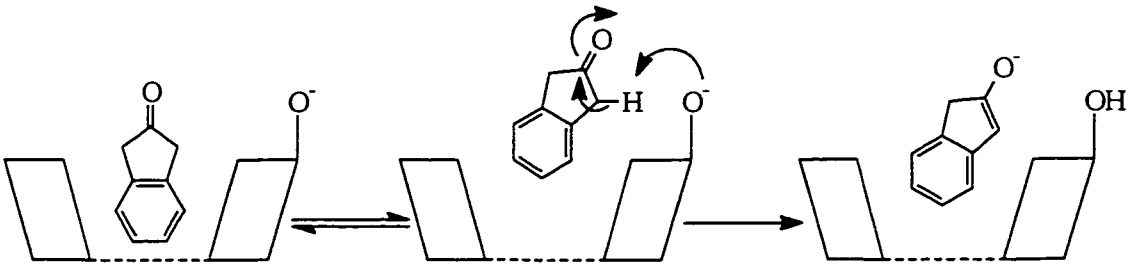

Scheme 1.2b Mechanism for catalysed enolization by β- and γ-CDs.

1.4.6 Cleavage of Phenyl Esters by Cyclodextrins

Acceleration of the cleavage of phenyl esters by cyclodextrins are in most cases established through covalent bond formation.[1-5,39,40] The magnitude of the "catalytic effect" is dependent on both the structure of the ester and the cyclodextrin. Normally, cleavage of the esters by cyclodextrins involves initial association of the esters with the cyclodextrins to form non-covalent 1:1 (ester:CD) complexes, followed by nucleophilic attack of ionized secondary hydroxyl groups on the carbonyl carbons of the esters to form tetrahedral intermediates, which

subsequently break down into phenols and acylated cyclodextrins. The acylated cyclodextrins are then slowly hydrolyzed,[39b] regenerating the cyclodextrins, so that the overall cleavage process is not truly catalysed. The kinetic parameters for the cleavage of some phenyl acetates by α-CD in aqueous buffer, pH 10.6 are given in Table 1.5.[1,39a]

Table 1.5 Kinetic parameters for cleavage of phenyl acetates by α-CD.[a]

Substituent	k_u ($10^{-4}s^{-1}$)	k_c ($10^{-2}s^{-1}$)	K_s (mM)	k_c/k_u	K_{ts} (mM)	*m/p*[b]
H	8.04	2.19	22	27.2	0.809	
m-Me	6.96	6.58	17	94.5	0.180	28.5
p-Me	6.64	0.220	11	3.31	3.32	
m-*t*-Bu	4.90	12.9	2.0	263	0.0076	239
p-*t*-Bu	6.07	0.067	6.5	1.1	6.50	
m-NO_2	14.0	42.5	19	303	0.063	86.7
p-NO_2	69.4	2.43	12	3.50	3.43	
m-CO_2^-	8.15	5.55	105	68.1	1.54	12.7
p-CO_2^-	12.5	0.67	150	5.36	28.0	

[a] From reference 1 & 39a. [b] Calculated as: $m/p = (k_c/k_u)_{meta}/(k_c/k_u)_{para}$

The data clearly show that *m*-substituted phenyl acetates are cleaved much better by α-CD than their *p*-substituted counterparts. The accelerations, k_c/k_u, obtained with the *m*-isomers, fall in the range 68 - 300, while those of the *p*-isomers are only between 1 and 6. The differences in the magnitudes of the accelerations are attributed to the differences in transition state binding, since substrate binding for each pair of isomers is about the same. The

transition state binding for the *m*-substituted phenyl esters is far superior (lower K_{ts} values) to that of their *p*-substituted analogues (higher K_{ts} values). Also noticeable, is the fact that the *meta/para* selectivity is more significant for esters with bulky substituents. Apparently, bulky substituents in the *meta* position leads to stronger transition state binding. Interestingly, the reactivity of the unsubstituted phenyl acetate lies between those of the *m*-, and *p*-substituted phenyl acetates.

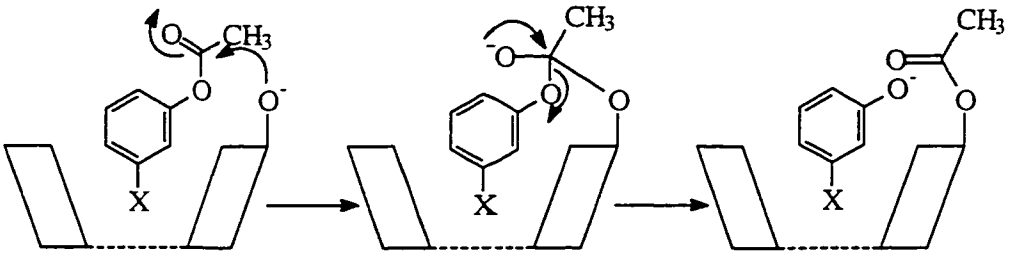

Scheme 1.3a Cleavage of *m*-substituted phenyl acetates by cyclodextrins.

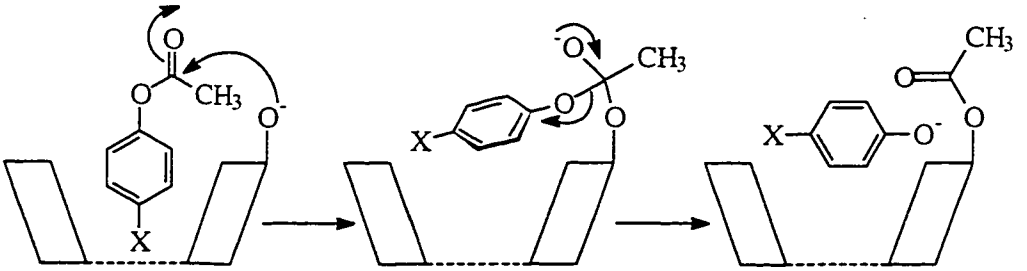

Scheme 1.3b Cleavage of *p*-substituted phenyl acetates by cyclodextrins.

The *meta/para* selectivity is believed to be due to the different geometries of the inclusion complexes formed.[1,5,21,39a] As shown in Scheme 1.3a, the carbonyl functional group of the ester is positioned in close proximity to the secondary hydroxyl groups on the cyclodextrin in the *m*-substituted phenyl acetate complex, which facilitates nucleophilic attack and subsequent formation of the tetrahedral intermediate. In a *p*-substituted phenyl acetate

complex (Scheme 1.3b), the carbonyl group extends into the bulk aqueous medium, farther away from the secondary hydroxyl groups which means that a considerable conformational change must take place for nucleophilic attack and consequent formation of the tetrahedral intermediate to occur.

The *meta/para* selectivity observed with α-CD is also seen with β-CD, although to a lesser extent.[39a] The accelerations attained for the *m*-esters with β-CD are not as large as those with α-CD, but the *p*-esters are cleaved better. The reduced *meta/para* selectivity has been attributed to the looser fit of the phenyl ring in the β-CD cavity. So far, the *meta/para* distinction observed for the cleavage of phenyl acetates by the smaller cyclodextrins seem to be non-existent in the case of γ-CD,[40] although only few data are available. The lack of selectivity is again probably due to the very loose fit provided by the γ-CD cavity.

Hammett-type plots of k_{obs}/k_u versus the substituent constant, σ, for the hydrolysis of some substituted phenyl acetates in the absence and presence of 10 mM α-, β-, and γ-CDs were constructed.[39a] Similar plots were constructed for the hydrolysis of the esters in the presence of glucose and methyl glucoside, and good linear correlations were obtained for these. However, there was absolutely no correlation for hydrolysis in the presence of cyclodextrins. The plots showed tremendous scatter indicating that the electronic nature of the substituents on the phenyl ring has little or no bearing whatsoever on the accelerations imposed by cyclodextrins.

The effects of acyl chain length on the cleavage of *m*-nitrophenyl,[42] and *p*-nitrophenyl alkanoates [41,42] by α-CD and β-CD have been studied. The *meta/para* selectivity observed with substituted phenyl acetates,[39a] is maintained throughout the series acetate to hexanoate,

although it tended to decrease with increasing acyl chain length. The trends in K_s with acyl chain length for both series of esters seem to indicate that after the acetate, there is a switch in the mode of substrate binding from aryl inclusion **8**, to acyl chain inclusion **9**. The trends in K_{ts} with acyl chain length indicate that the transition state binding involves inclusion of the acyl chain for the *p*-nitrophenyl alkanoates whereas aryl inclusion is dominate for the *m*-nitrophenyl alkanoates. For the cleavage of these nitrophenyl alkanoates by γ-CD, the K_s and K_{ts} values seem to be independent of acyl chain length, indicating that aryl inclusion is probably dominant in both the initial and transition states.[40]

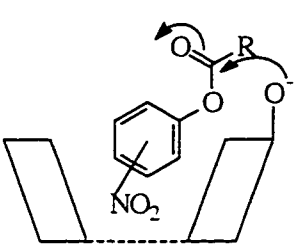

8

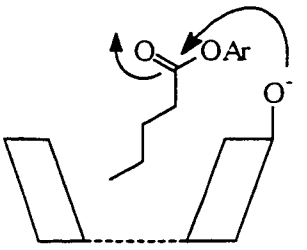

9

The cleavage of phenyl esters by cyclodextrins in aqueous solution usually exhibits simple saturation-type kinetics involving the formation of 1:1 (ester:CD) complexes.[1,2,5,39-42] However, there have been cases where an additional process involving a second CD molecule becomes apparent at higher CD concentrations.[43-45] For example, the cleavage of 2-carboxy-4-nitrophenyl and 4-carboxy-2-nitrophenyl alkanoates with long acyl chains (C_3-C_8) by α-CD and β-CD exhibited a variety of behaviours including acceleration and retardation, retardation and acceleration, and two types of acceleration.[43] These behaviours were rationalized by relatively simple reaction schemes. In the case of acceleration followed by retardation, the

second CD molecule binds to the productive 1:1 (ester:CD) complex to form a non-productive 2:1 (CD:ester) complex. In the cases of retardation followed by acceleration, and acceleration followed by another type of acceleration, the second CD molecule may act as a nucleophile, attacking the 1:1 (ester:CD) complex **10**, or it may form a productive 2:1 (CD:ester) ternary complex **11** within which the cleavage reaction occurs. Two types of acceleration were also observed for the cleavage of *p*-nitrophenyl alkanoates with long acyl chains by hydroxypropyl-β-CD where, as in the previous cases, the second CD molecule acts either as a nucleophile attacking a productive 1:1 complex, or forms a ternary complex within which the reaction occurs.[44] Very recently, evidence was sought and found of ester cleavage involving two different cyclodextrins.[45]

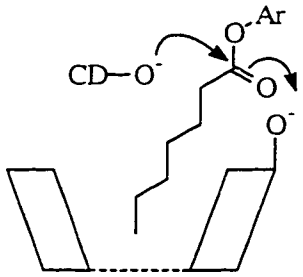

10

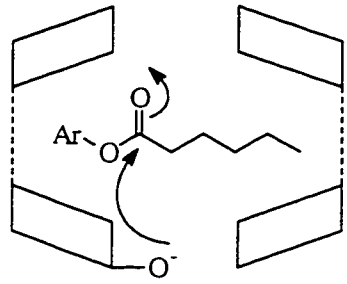

11

2. RESULTS and DISCUSSION

The hydrolytic cleavage of *p*-nitrophenyl esters of N-*tert*-butyloxycarbonyl amino acids (BOC-Esters, **I**) and N-benzyloxycarbonyl amino acids (CBZ-Esters, **II**) in basic aqueous solution containing cyclodextrins (i.e., α-CD, β-CD or γ-CD) was studied in this work. The structures of the amino acid side chains are shown in Figure 2.1. In addition, the cleavage of *p*-nitrophenyl esters of BOC-β-Ala, **III**, CBZ-β-Ala, **IV**, and CBZ-Gly-Gly, **V**, as well as an enantiomeric pair of N-hydroxysuccinimide esters of BOC-Pro, **VI**, was studied.

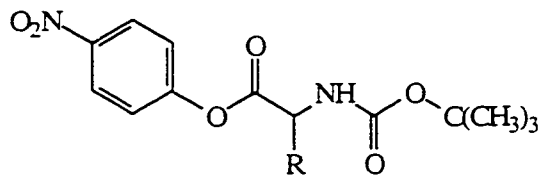

I

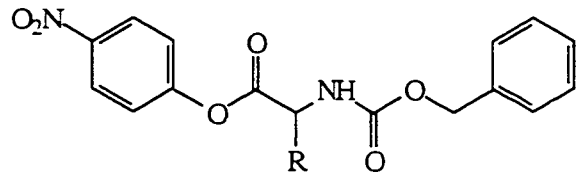

II

Gly	—H	Ile	—$CH(CH_3)CH_2CH_3$
Ala	—CH_3	Val	—$CH(CH_3)_2$
Met	—$CH_2CH_2SCH_3$	Asn	—CH_2CONH_2
Leu	—$CH_2CH(CH_3)_2$	Gln	—$CH_2CH_2CONH_2$
Phe	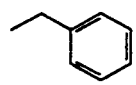	Trp	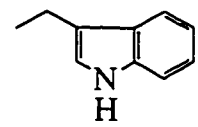

Figure 2.1 Structures of amino acid side chains.

The carbamate group (-NHCOO-) of these esters is relatively insensitive to nucleophilic attack due to resonance stabilization involving the lone pair of electrons on the nitrogen.[47,48] Thus, in comparison to the ester function, the carbamate group is relatively stable to alkaline hydrolysis in basic solution. Likewise, the imide group in the succinimide ring of **VI** is fairly resistant to alkaline hydrolysis compared with the ester function.[47]

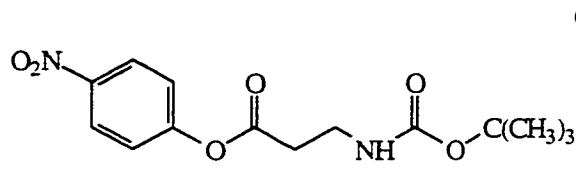

III

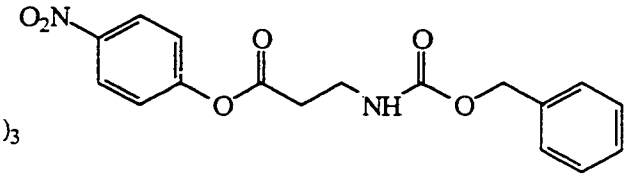

IV

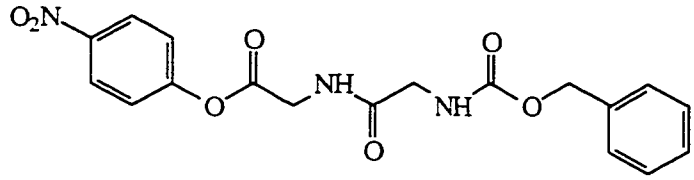

V

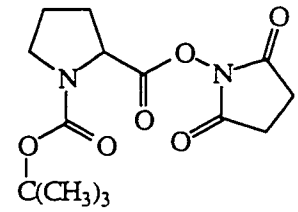

VI

The kinetics of cleavage of the esters described above in the presence of CDs were measured by uv-vis stopped-flow spectrophotometry. Pseudo first-order rate constants, k_{obs}, for cleavage of the *p*-nitrophenyl esters were obtained over a range of $[CD]_o$ by following the appearance of the *p*-nitrophenolate anion at 405 nm. The kinetics of cleavage of the pair of N-hydroxysuccinimide esters were monitored at 231 nm. The kinetic data obtained are collected in the Appendix. Also, since the cleavage process usually involves formation of ester/CD complexes, circular dichroism studies were carried out to help elucidate the dominant mode of binding of the esters in these complexes.

Circular dichroism (c.d.) is induced in the absorption bands of an achiral chromophore when it binds to the asymmetric cavity of a cyclodextrin.[50-55] Electronic transition moments polarized along the long axis of mono- and *para*-substituted phenyl derivatives, which are parallel to the C_n symmetry axis of the cyclodextrin, (Figure 2.2a), show positive induced c.d., while transition moments polarized along the short axis of these phenyl derivatives, which are

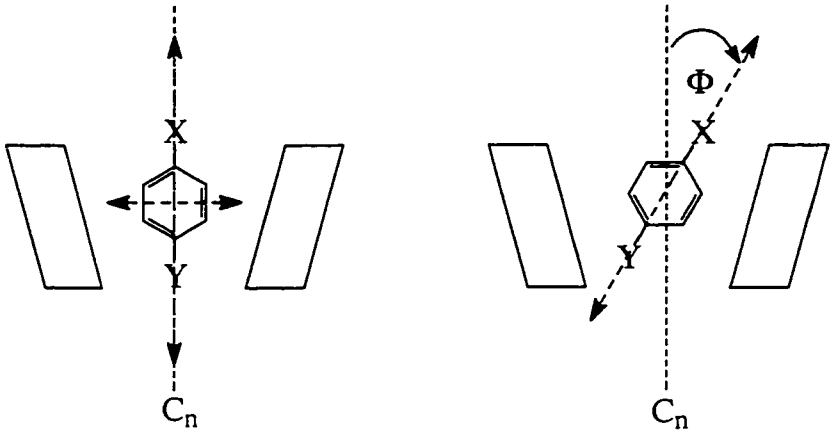

(a) (b)

Figure 2.2 Orientations of transition moments of *p*-substituted phenyl derivatives.

perpendicular to the C_n symmetry axis, show negative induced c.d.[53] The intensity of the induced c.d. decreases as the angle, Φ, (Figure 2.2b) increases and at an angle somewhere between 30 and 40°, the induced c.d. signal eventually vanishes.[54] Similarly, electric transition moments of other aromatic guests, parallel to the C_n symmetry axis show positive induced c.d. while those perpendicular show negative induced c.d.[50-52,54] Recently, Kodaka proposed a new rule for predicting the sign of the induced c.d. of an achiral chromophore located outside the cyclodextrin cavity[55] based on the Kirkwood-Tinoco equation.[67]

The induced c.d. spectra of *p*-nitrophenyl acetate (*p*NPA) with α-, β-, and γ-CDs in

water containing 0.1% acetonitrile are shown in Figure 2.3. As seen in the figure, the ester on its own does not exhibit circular dichroism, however, in the presence of cyclodextrins, circular dichroism is induced. The induced c.d. spectrum of *p*NPA with α-CD has a positive peak at about 285 nm, and a negative peak at 220 nm with a shoulder at 238 nm. With β-CD, a positive peak is observed at about 271 and a negative peak at around 215 nm. There also seems to be a weak shoulder at about 240 nm. For *p*NPA with γ-CD, a weak positive induced c.d. signal with a peak at about 273 nm is observed.

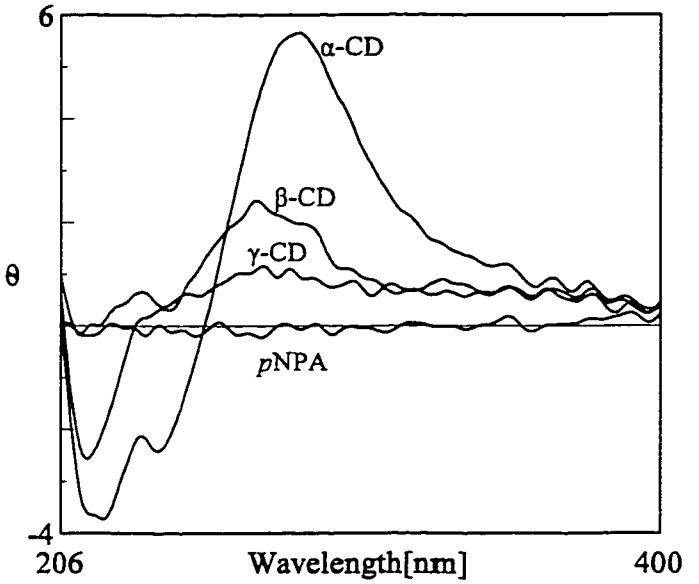

Figure 2.3 Induced c.d. spectra for 0.1 mM *p*NPA with 20 mM α-CD,10 mM β-CD, and 50 mM γ-CD.

2.1 Structure-Activity Analysis for Ester Cleavage by α-CD

Rate data for cleavage of the BOC-Esters by α-CD conform to simple saturation kinetics as shown in Figure 2.4. This behaviour is consistent with cleavage of the esters, S, in buffer, (2.1), and through 1:1 (ester:CD) complexes, S.CD, (2.2), to give products. As a result, the dependence of k_{obs} on $[CD]_o$ is described by equation (2.3). The k_u values were measured directly in buffer, while the k_c and K_s values were determined by non-linear fitting of equation (2.3). The k_u, k_c, and K_s values obtained, along with the calculated constants k_2, k_c/k_u, and K_{ts} are given in Table 2.1.

$$S \xrightarrow{k_u} P \qquad (2.1)$$

$$S + CD \underset{K_s}{\rightleftharpoons} S.CD \xrightarrow{k_c} P \qquad (2.2)$$

$$k_{obs} = \frac{k_u K_s + k_c [CD]_o}{K_s + [CD]_o} \qquad (2.3)$$

Rate data for cleavage of the esters CBZ-Gly, CBZ-β-Ala, and CBZ-Gly-Gly by α-CD also satisfy equation (2.3). However, the dependence of k_{obs} on $[CD]_o$ for cleavage of the other CBZ-Esters is linear, indicative of very weak (i.e., $K_s >> [CD]_o$) or no binding (Figure 2.5). Thus, the cleavage process is better represented by (2.1) and (2.4), and the kinetics described by equation (2.5). The k_2 values were obtained from the slopes of the plots of k_{obs} versus $[CD]_o$ and are also given in Table 2.1, along with the k_u and K_{ts} values.

$$S + CD \xrightarrow{k_2} P \qquad (2.4)$$

$$k_{obs} = k_u + k_2 [CD]_o \qquad (2.5)$$

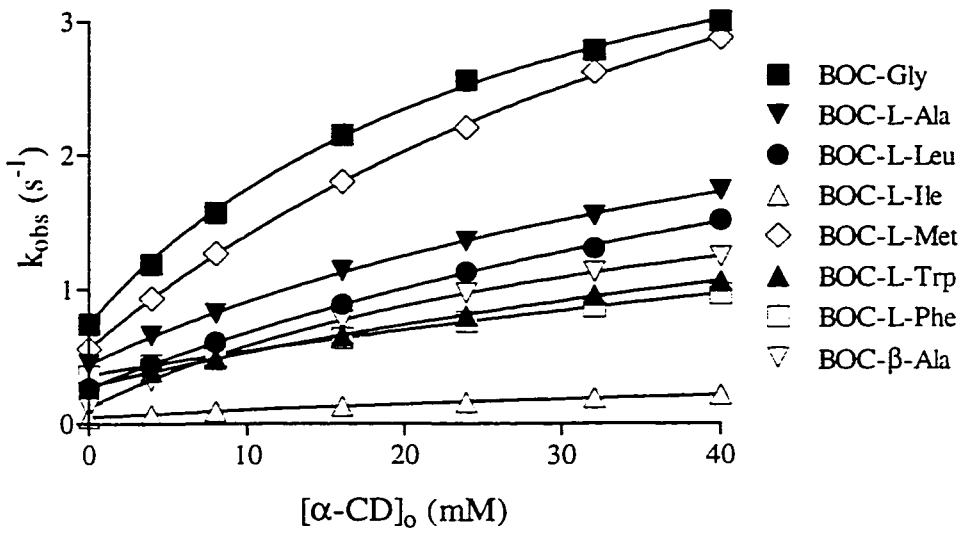

Figure 2.4 Plots of k_{obs} vs $[\alpha\text{-CD}]_o$ for cleavage of BOC-Esters.

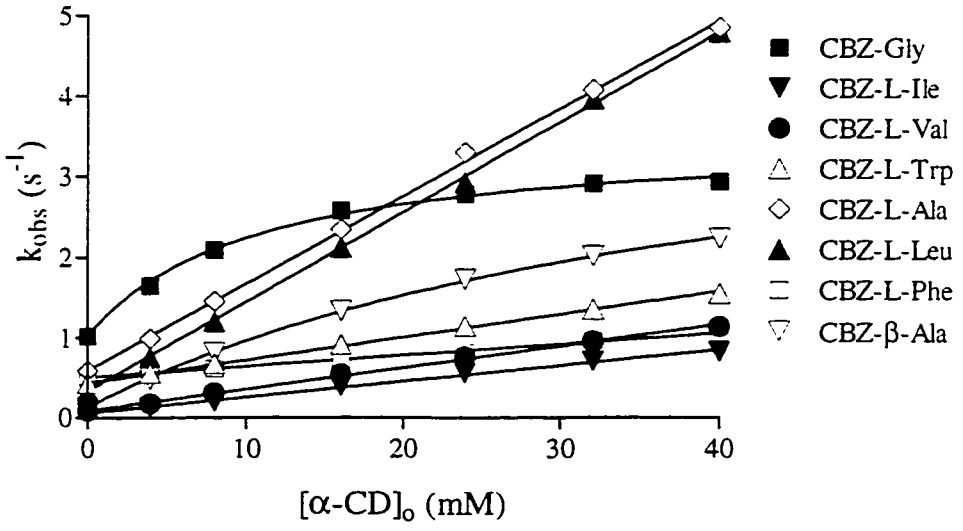

Figure 2.5 Plots of k_{obs} vs $[\alpha\text{-CD}]_o$ for cleavage of CBZ-Esters.

Table 2.1 Constants for Cleavage of Esters by α-CD.[a]

Ester	k_u s^{-1}	K_s mM	k_c s^{-1}	k_c/k_u	k_2 $M^{-1}s^{-1}$	K_{ts} mM
BOC-Esters with α-CD						
Gly	0.746	28.9 ± 1.9	4.65 ± 0.14	6.26	161	4.62
L-Ala	0.447	55.8 ± 3.5	3.50 ± 0.13	7.83	62.7	7.13
L-Met	0.560	55.4 ± 3.6	6.09 ± 0.24	10.9	110	5.09
L-Leu	0.267	77.1 ± 7.1	3.88 ± 0.24	14.5	50.3	5.31
L-Ile	0.0491	81.6 ± 6.5	0.553 ± 0.030	11.3	6.78	7.25
L-Trp[b]	0.283	97.0 ± 8.9	2.96 ± 0.19	10.5	30.5	9.27
L-Phe[c]	0.365	153 ± 15	3.28 ± 0.23	8.99	21.4	17.0
β-Ala	0.120	36.8 ± 0.9	2.28 ± 0.03	19.0	62.0	1.94
CBZ-Esters with α-CD						
Gly	1.02	10.4 ± 1.05	3.51 ± 0.09	3.44	338	3.03
L-Ala	0.590				108	5.46
L-Leu	0.356				112	3.18
L-Val	0.0874				26.6	3.29
L-Ile	0.0599				19.8	3.03
L-Trp[b]	0.437				27.9	15.7
L-Phe[c]	0.509				13.8	36.8
β-Ala	0.130	40.9 ± 2.6	4.42 ± 0.16	34.0	108	1.20
Gly-Gly	4.68	85.1 ± 8.5	84.1 ± 5.8	18.0	988	4.74

[a] At 25 °C, in 0.2 M phosphate buffer, pH 11.6 containing 0.1%, [b] 5%, and [c] 10% acetonitrile. $k_2 = k_c/K_s$, $K_{ts} = k_uK_s/k_c$ or k_u/k_2.

As seen in Figures 2.4 and 2.5, cleavage of the BOC- and CBZ-Esters is modestly enhanced by α-CD. The maximal accelerations, k_c/k_u, achieved with the BOC-Esters are fairly constant, ranging in magnitudes from 6 to 11 in most cases. The constant accelerations are due to the fact that the trends in K_s, essentially parallel those in K_{ts}, since as explained earlier $k_c/k_u = K_s/K_{ts}$ (Section 1.4.2). Apart from CBZ-Gly, CBZ-β-Ala, and CBZ-Gly-Gly, values of k_c/k_u for cleavage of the CBZ-Esters could not be determined since saturation kinetics were not observed. Interestingly, the best accelerations within each of the two series are achieved with the β-Ala esters which are due primarily to stronger transition state binding.

The k_u values, which are measures of intrinsic reactivities, reflect the inherent steric and electronic characteristics of the esters. These characteristics are sometimes seen in the k_2 values, along with the effects of the cyclodextrin. The trends in the k_2 values for both the BOC- and CBZ-Esters generally parallel those in the k_u values as seen in the plots of log k_2 versus log k_u (Figures 2.6 and 2.7) indicating that the reactivities of the esters in each series with α-CD, and hence the strengths of transition state binding, are about the same. The deviant points for the β-Ala esters indicate that they are more reactive with α-CD, while those for the Trp and Phe esters suggest that they are less reactive. Thus, it seems as though the presence of the additional methylene group between the carbamate and ester functions of the β-Ala esters improves reactivity with α-CD, while the bulky indolyl and phenyl rings in the amino acid side chains of the Trp and Phe esters respectively, lessen reactivity. Unfortunately, the reduced reactivity of these last two esters may have been magnified by the higher acetonitrile content needed to dissolve them in the aqueous medium.

The K_s values for the BOC-Esters generally tends to increase with the bulkiness of the

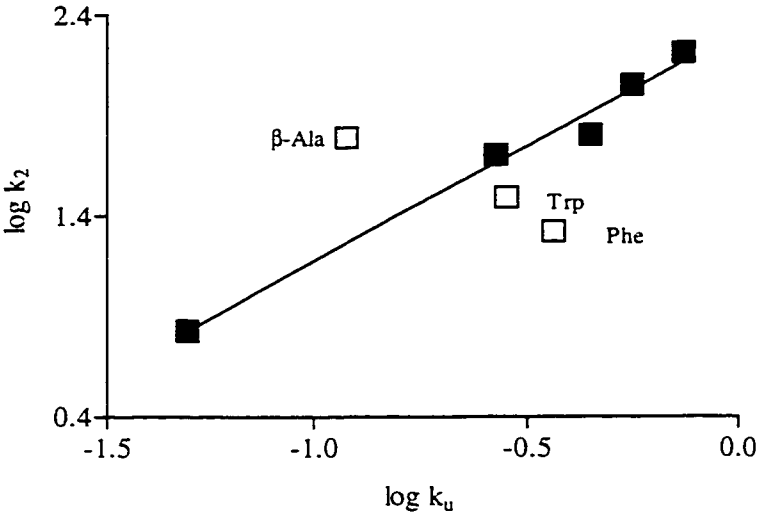

Figure 2.6 Plot of log k_2 vs log k_u for BOC-Esters with α-CD. Linear regression analysis done with ■ only. (Slope = 1.13 ± 0.08; r = 0.992)

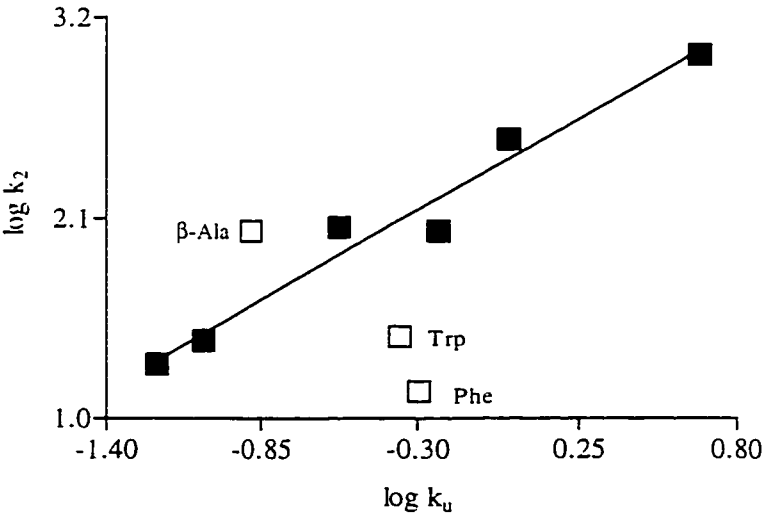

Figure 2.7 Plot of log k_2 vs log k_u for CBZ-Esters with α-CD. Linear regression analysis done with ■ only. (Slope = 0.896 ± 0.083; r = 0.983)

amino acid side chains, indicating that substrate binding becomes weaker (Table 2.1). However, for the CBZ-Esters, K_s values were only obtained for CBZ-Gly, CBZ-β-Ala, and CBZ-Gly-Gly which do not have any amino acid side chains. Substrate binding was not detected for the other CBZ-Esters and hence, no K_s values were obtained. The induced c.d. spectra obtained for the achiral esters of BOC-Gly, BOC-β-Ala, CBZ-Gly, and CBZ-β-Ala with α-CD, are identical to that seen for *p*NPA with α-CD (Figure 2.8), indicating that substrate binding involves inclusion of the *p*NP group. Moreover, the peak for the inherent c.d. spectrum of BOC-L-Ala is quenched upon addition of α-CD, and induced c.d. peaks appear which virtually mirror those seen for *p*NPA with α-CD (Figure 2.9), indicating that the *p*NP group resides inside the α-CD cavity. Thus, the dominant mode of substrate binding for both series of esters seems to involve inclusion of the *p*NP group. The presence of amino acid side chains appears to hinder binding of the *p*NP group in the case of the BOC-Esters while for the CBZ-Esters, the side chains seem to result in a conformational change which causes the CBZ-group to hinder binding of the *p*NP moiety.

In general, the K_{ts} values for the BOC-Esters, as well as those for the CBZ-Esters, do not vary much. Moreover, the K_{ts} values for the two series of esters are fairly comparable to each other, and to that of *p*NPA which is 3.6 mM,[5,42] suggesting that the *p*NP group resides inside the α-CD cavity during the transition state binding. The K_{ts} values for the Trp and Phe esters are appreciably higher than those of the other esters indicating that transition state binding is much weaker. Apparently, the bulky amino acid side chains of these last two esters reduce the depth of penetration of the *p*NP group which result in weaker transition state binding, since it is improbable that they would switch to a less stable mode of transition state

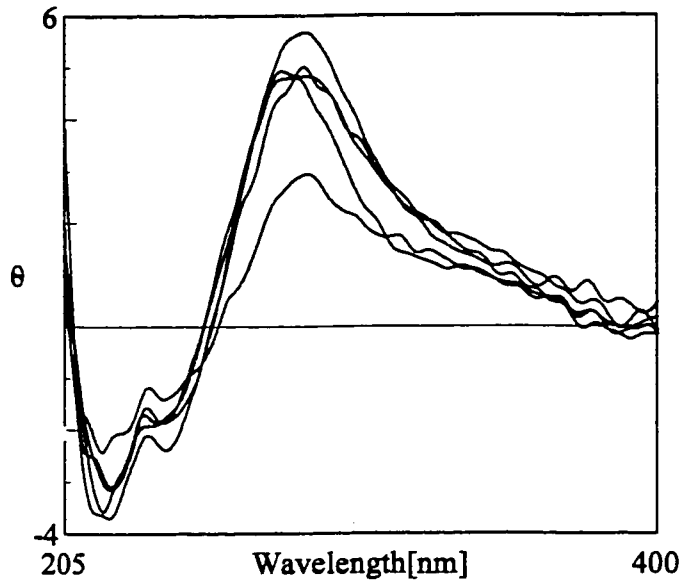

Figure 2.8 Induced c.d. spectra of *p*NPA with 20 mM α-CD, and BOC-Gly, CBZ-Gly, BOC-β-Ala, and CBZ-β-Ala with 40 mM α-CD.

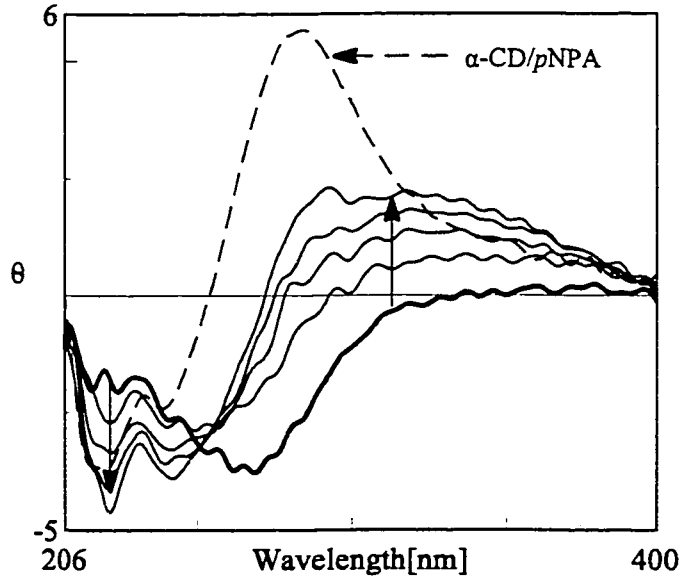

Figure 2.9 Effect of 0, 10, 20, 30, and 40 mM α-CD on c.d. spectrum of BOC-L-Ala. Arrows indicate effect of increasing $[\alpha\text{-CD}]_o$.

binding. In the case of the β-Ala esters, the additional methylene group between the carbamate and ester functions results in the carbonyl carbon being spatially less crowded, thus facilitating formation of the transition states. A plot of the pK_{ts} values[b] for the CBZ-Esters versus those of the corresponding BOC-Esters is shown in Figure 2.10. The linear correlation obtained indicates that the transition state structures for the two series of esters are quite similar. However, the fact that the slope is greater than unity may be an indication that the transition state geometries for the two series of esters are slightly different.

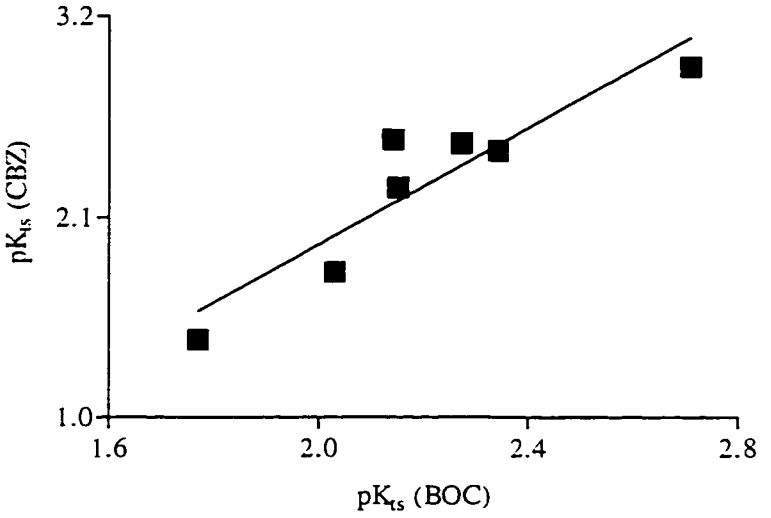

Figure 2.10 pK_{ts} values for CBZ-Esters vs BOC-Ester with α-CD. (Slope = 1.59 ± 0.30; r = 0.920)

[b] $\Delta G^{\circ}_{ts} = 2.303\ RT\ pK_{ts}$; $\Delta G^{\circ}_{s} = 2.303\ RT\ pK_{s}$

2.2 Structure-Activity Analysis for Ester Cleavage by β-CD

The dependence of k_{obs} on $[CD]_o$ for cleavage of the BOC-Esters by β-CD does not follow simple saturation kinetics since k_{obs} increases linearly with higher $[CD]_o$ (Figure 2.11). The kinetics are consistent with the processes (2.1) and (2.2), along with a third process involving the reaction of free CD molecules with 1:1 S.CD complexes, (2.6). Thus, the dependence of k_{obs} on $[CD]_o$ is described by equation (2.7). The fitted constants K_s, k_c, and k_{c2}, as well as the calculated constants k_c/k_u, k_2, K_{ts}, and K'_{ts} are given in Table 2.2. The significance of k_{c2} and K'_{ts} will be discussed later in this section.

$$S.CD + CD \xrightarrow{k_{c2}} P \qquad (2.6)$$

$$k_{obs} = \frac{k_u K_s + k_c[CD]_o + k_{c2}[CD]_o^2}{K_s + [CD]_o} \qquad (2.7)$$

For cleavage of the CBZ-Esters by β-CD, the dependence of k_{obs} on $[CD]_o$ corresponds to saturation kinetics which is consistent with the processes (2.1) and (2.2). Therefore, the dependence of k_{obs} on $[CD]_o$ is adequately described by equation (2.3). The kinetic parameters obtained are also given in Table 2.2.

Generally speaking, the accelerations, k_c/k_u, for cleavage of the BOC-Esters are comparable to those of the corresponding CBZ-Esters (Table 2.2), although they are slightly larger for the CBZ-Esters. Furthermore, the trends in the k_c/k_u values for the two series of esters are quite similar. The differences in the accelerations within each series of esters are due mainly to differences in the K_s values, since the K_{ts} values for most of the esters are essentially the same.

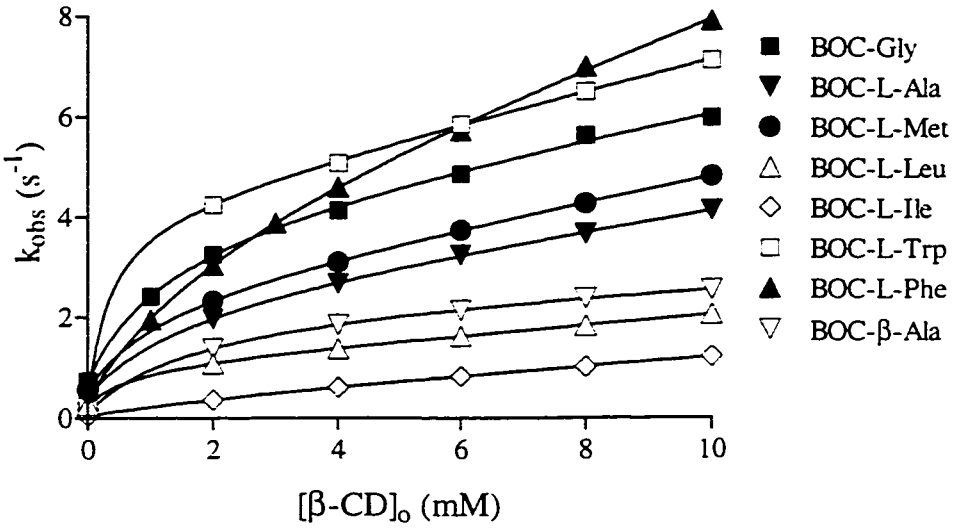

Figure 2.11 Plots of k_{obs} vs $[\beta\text{-CD}]_o$ for cleavage of BOC-Esters.

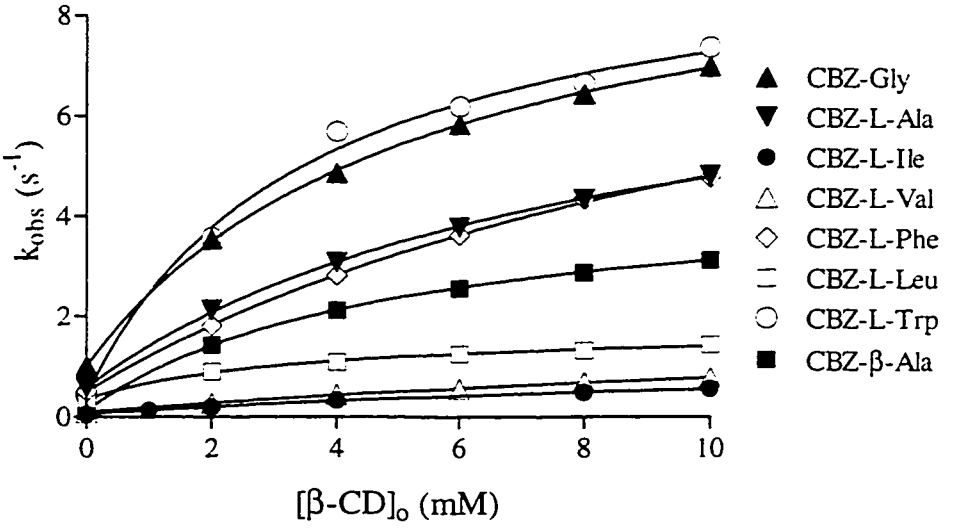

Figure 2.12 Plots of k_{obs} vs $[\beta\text{-CD}]_o$ for cleavage of CBZ-Esters.

Table 2.2 Constants for Cleavage of Esters by β-CD.[a]

Ester	K_s mM	k_c s^{-1}	k_c/k_u	k_2 $M^{-1}s^{-1}$	K_{ts} mM	k_{c2} $M^{-1}s^{-1}$	K'_{ts} mM
BOC-Esters with β-CD							
Gly	1.32 ± 0.35	4.41 ± 0.49	5.91	3330	0.223	233 ± 37	18.9
L-Ala	1.71 ± 0.30	2.92 ± 0.23	6.53	1700	0.262	183 ± 13	16.0
L-Met	1.26 ± 0.09	2.97 ± 0.08	5.30	2360	0.238	237 ± 5	12.5
L-Leu	0.803 ± 0.105	1.22 ± 0.04	4.57	1510	0.176	98.1 ± 0.3	12.4
L-Ile	4.42 ± 1.61	0.894 ± 0.255	18.2	202	0.243	83.9 ± 0.7	10.7
L-Trp[b]	0.335 ± 0.066	4.30 ± 0.14	15.2	12800	0.022	306 ± 11	14.1
L-Phe[c]	2.34 ± 0.48	5.30 ± 0.68	14.5	2270	0.161	439 ± 36	12.1
β-Ala	1.82 ± 0.15	2.41 ± 0.10	20.1	1330	0.091	57.5 ± 0.7	41.9
CBZ-Esters with β-CD							
Gly	5.29 ± 0.21	10.1 ± 0.2	9.90	1910	0.534		
L-Ala	8.13 ± 0.38	8.16 ± 0.19	13.8	1000	0.587		
L-Leu	3.36 ± 0.38	1.76 ± 0.06	4.95	524	0.679		
L-Val	18.9 ± 2.1	2.09 ± 0.16	23.9	111	0.791		
L-Ile	14.1 ± 1.8	1.27 ± 0.10	21.2	90.1	0.665		
L-Trp[b]	3.53 ± 0.63	9.66 ± 0.61	22.1	2740	0.160		
L-Phe[c]	12.9 ± 0.9	10.4 ± 0.4	20.4	805	0.638		
β-Ala	4.80 ± 0.08	4.54 ± 0.03	34.9	946	0.137		
Gly-Gly	4.15 ± 0.22	37.9 ± 0.7	8.49	9140	0.488		

[a] At 25 °C, in 0.2 M phosphate buffer, pH 11.6 containing 0.1%, [b] 5%, and [c] 10% acetonitrile. k_u values are given in Table 2.1. $k_2 = k_c/K_s$, $K_{ts} = k_u K_s/k_c$, and $K'_{ts} = k_c/k_{c2}$.

The k_2 values obtained for the BOC-Esters are higher than those determined for the corresponding CBZ-Esters, indicating that they are more reactive with β-CD. This greater reactivity is due to stronger transition state binding of the BOC-Esters to the CD. However, both series of esters are significantly more reactive with β-CD than they are with α-CD. The plots of log k_2 versus log k_u (Figures 2.13 and 2.14) show that the reactivities of most of the esters in each series with β-CD are quite similar, suggesting that transition state binding is essentially the same. In both series, the Trp and β-Ala esters are the most reactive with β-CD, and this is again due to better transition state binding (Figures 2.15 and 2.16).

The K_s values for the BOC-Esters are generally lower than those for the CBZ-Esters implying that they bind a lot stronger to β-CD. Also, the K_s values for both series of esters with β-CD are substantially lower than those seen with α-CD (Table 2.1). K_s values obtained in previous work for the binding of *p*NPA to β-CD are 6.1,[39a] 6.5,[41] and 7.8 mM,[42] which are higher than those obtained with the BOC-Esters, but comparable somewhat to those seen with the CBZ-Esters. As well, the intensities of the induced c.d. peaks obtained for BOC-Gly with β-CD are much weaker than those obtained for CBZ-Gly and *p*NPA (Figure 2.18). These observations may be an indication that the BOC-Esters generally bind by the BOC-group, while the CBZ-Esters bind by the *p*NP group. The fluctuations in the K_s values and hence, pK_s values (Figures 2.15 and 2.16), likely result from steric and/or conformational effects due to the different amino acid side chains which affect binding of the respective BOC- and *p*NP groups. In fact, for most of the esters containing α-amino acids, a fairly good linear correlation exists between the pK_s values of the CBZ-Esters versus those of the corresponding BOC-Esters as shown in Figure 2.17, indicating that the amino acid side chains basically have

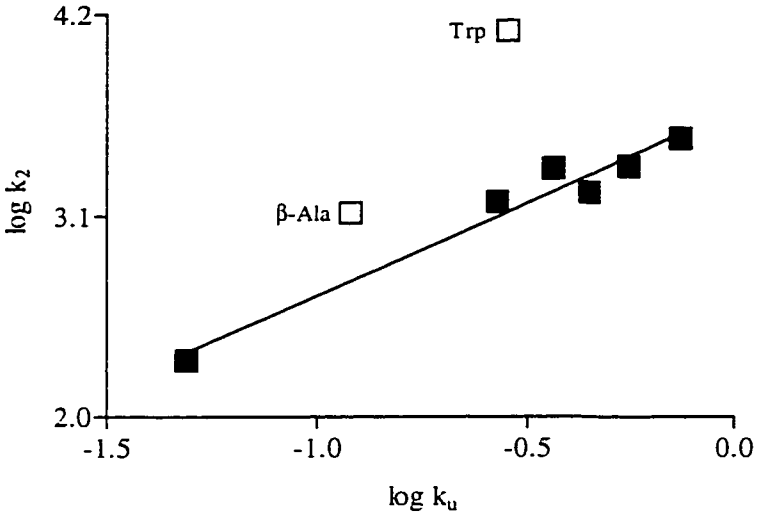

Figure 2.13 Plot of log k_2 vs log k_u for BOC-Esters with β-CD. Linear regression analysis done with ■ only. (Slope = 1.01 ± 0.10; r = 0.980)

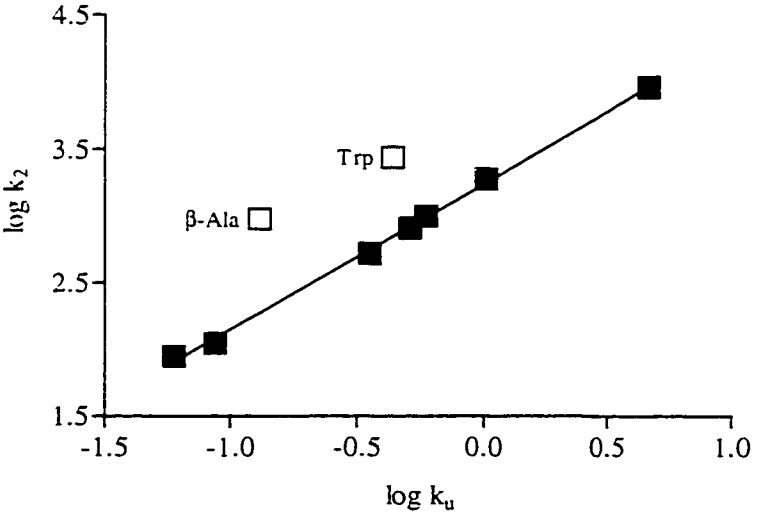

Figure 2.14 Plot of log k_2 vs log k_u for CBZ-Esters with β-CD. Linear regression analysis done with ■ only. (Slope = 1.09 ± 0.02; r = 0.999)

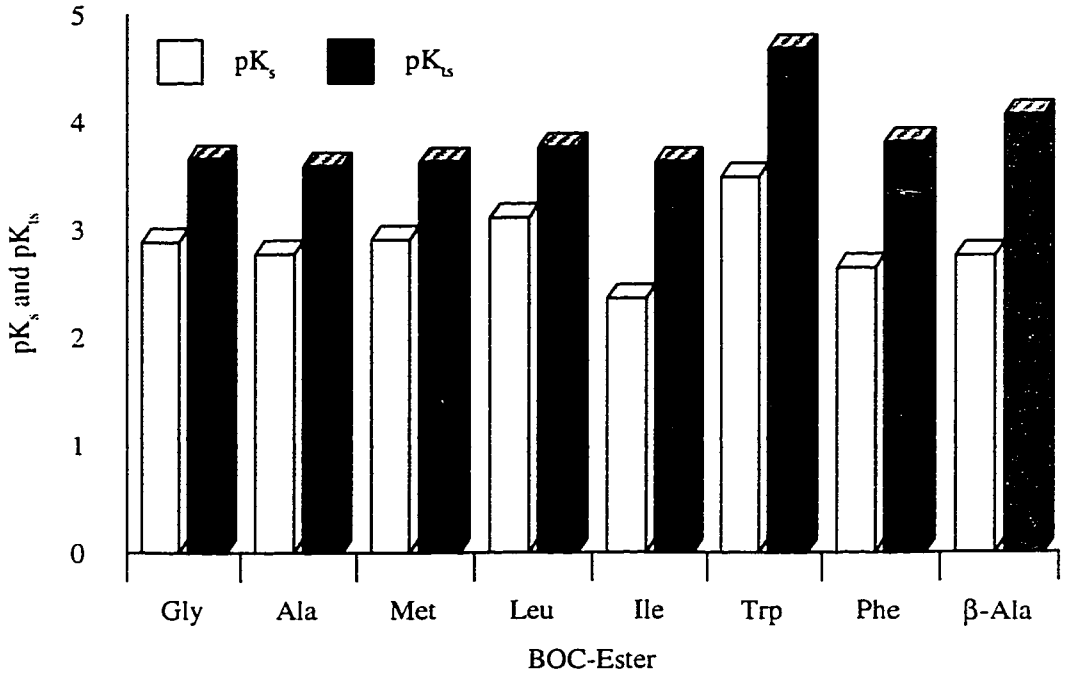

Figure 2.15 pK_s and pK_{ts} values for BOC-Esters with β-CD.

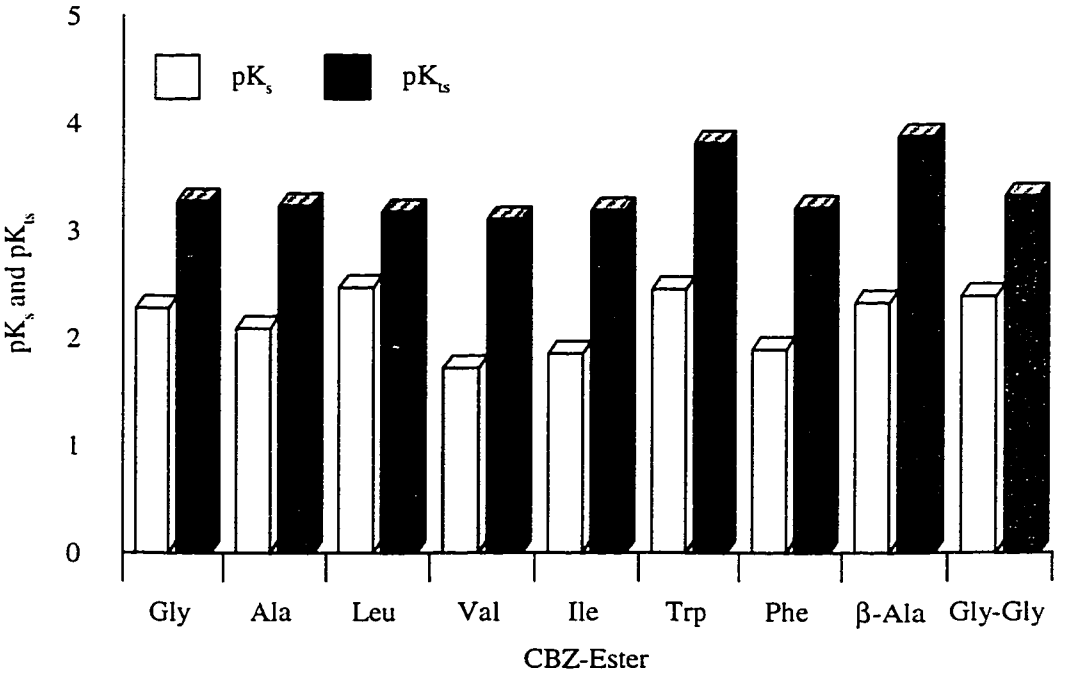

Figure 2.16 pK_s and pK_{ts} values for CBZ-Esters with β-CD.

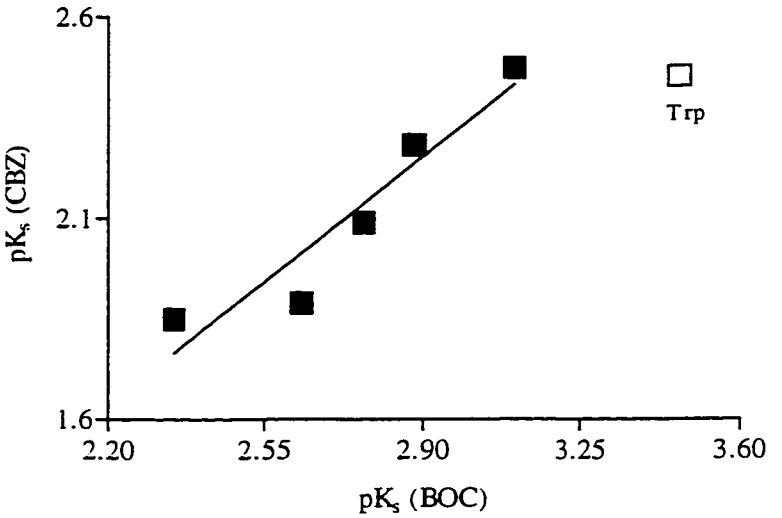

Figure 2.17 pK_s values for CBZ- vs BOC-Esters containing α-amino acids. Linear regression analysis done with ■ only. (Slope = 0.886 ± 0.173; r = 0.947)

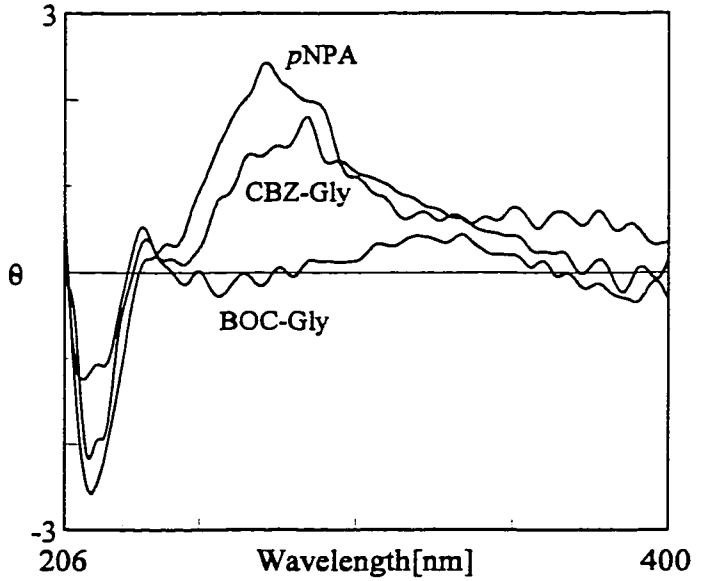

Figure 2.18 Induced c.d. spectra for CBZ-Gly and BOC-Gly with 5 mM β-CD, and pNPA with 10 mM β-CD.

the same effect on the binding of both series of esters. However, this linear relationship could very well mean that both series of esters bind to β-CD by the *p*NP group, but the CBZ-Esters bind weaker because of greater steric hindrance resulting from the bulkier CBZ-group. The K_s value for BOC-Trp is noticeably lower than those for the other BOC-Esters suggesting that this ester binds to β-CD by its indolyl ring. There is also a good possibility that CBZ-Trp binds to β-CD by the indolyl ring, but the binding may be hindered by the bulkier CBZ-group which results in the K_s value being about 10-fold higher than that for BOC-Trp.

The K_{ts} values for the BOC-Esters are also much lower than those for the CBZ-Esters which indicate that they bind a lot stronger to β-CD in the transition state. In addition, the K_{ts} values for both series of esters, and thus pK_{ts} values (Figures 2.15 and 2.16), are in most cases remarkably constant, suggesting that the transition state structures within each series are basically the same. Moreover, the K_{ts} values reported in earlier work for transition state binding of *p*NPA to β-CD are 0.67,[39a] 0.53,[41] and 0.96 mM,[42] which are higher than those obtained with the present BOC-Esters, but practically the same as those determined for the CBZ-Esters. These facts seem to suggest that transition state binding for the BOC-Esters generally involves inclusion of the BOC-group, while that for the CBZ-Esters involves inclusion of the *p*NP group. The higher pK_{ts} value for BOC-Trp (Figure 2.15) indicates that this ester binds to β-CD by the indolyl ring in the transition state, and this may also be the case for CBZ-Trp. Also, as seen earlier with α-CD, the K_{ts} values for the β-Ala esters with β-CD are noticeably lower (higher pK_{ts} values) than those for most of the other esters within their respective series, showing that the presence of the additional methylene group again facilitates formation of the transition state.

The second-order rate constant, k_{c2}, for the reaction of the S.CD complexes with free CD, equation (2.6), depends to some extent on the intrinsic reactivities of the esters. This means that k_{c2} does not necessarily convey the actual reactivity of the S.CD complexes with unbound CD; this reactivity is more accurately expressed by the ratio k_{c2}/k_c. Application of the Kurz approach[32,33] to the rate constants k_c and k_{c2} gives rise to equation (2.9) which defines a pseudo equilibrium constant, K'_{ts}, for dissociation of the ternary transition state complex, $TS.CD_2$, into TS.CD and CD, equation (2.8). It should be mentioned that the term, k'_c, in equation (2.9), is the limiting rate constant due to reaction within a $S.CD_2$ complex.

$$TS.CD + CD \xrightleftharpoons[K'_{ts}]{} TS.CD_2 \qquad (2.8)$$

$$k_c/k_{c2} = \frac{[TS.CD][CD]}{[TS.CD_2]} = K'_{ts} = k_c K_s/k'_c \qquad (2.9)$$

As illustrated in Figure 2.19, K'_{ts} essentially relays the extent to which the second CD stabilizes the transition state of the 1:1 cleavage process. The K'_{ts} values in Table 2.2, and thus the pK'_{ts} values (Figure 2.20), are fairly constant, except that for BOC-β-Ala which is about 2 - 3 times higher. This means that apart from BOC-β-Ala, the reactivities of the different S.CD complexes with free β-CD, and therefore the structures of the ternary transition state complexes, are very similar.

The reaction involving the S.CD complexes with unbound CD may generally occur as depicted in **12**, where the first CD binds to the BOC-group, and then the second CD attacks the ester within the S.CD complex. In the case of BOC-Trp, the first CD likely binds to the indolyl ring instead. However, the relatively low K'_{ts} values may be an indication that the

reactions occur within weak 1:2 (ester:CD), $S.CD_2$, complexes where the second CD binds to the *p*NP group as in **13** and **14**. There may also be a sort of cooperative-type behaviour between the two CDs as illustrated in **15** where one CD acts as a nucleophile, while the other acts as a general acid catalyst within a weak $S.CD_2$ complex. It is also possible that within the $S.CD_2$ complex, one CD forms the covalent tetrahedral intermediate, while the other CD stabilizes this anionic intermediate via hydrogen bonding. Unfortunately, it is difficult to decide which is the actual mechanism since they are all kinetically equivalent.

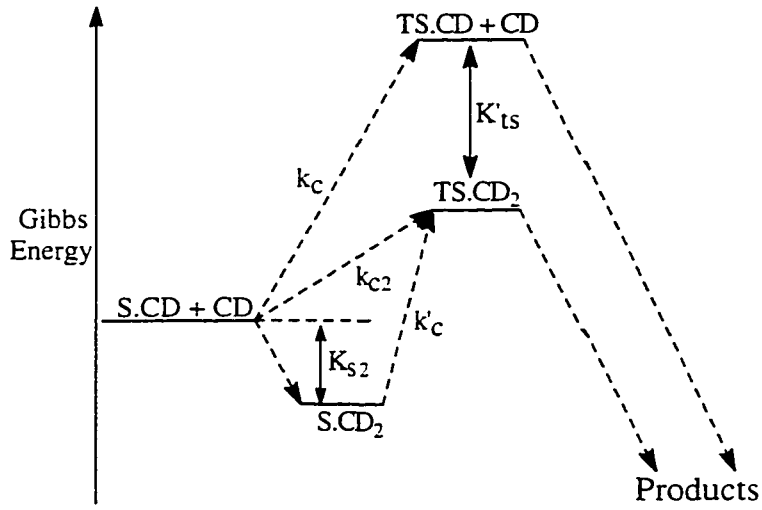

Figure 2.19 Gibbs free energy diagram showing the transition state stabilization by a second CD molecule.

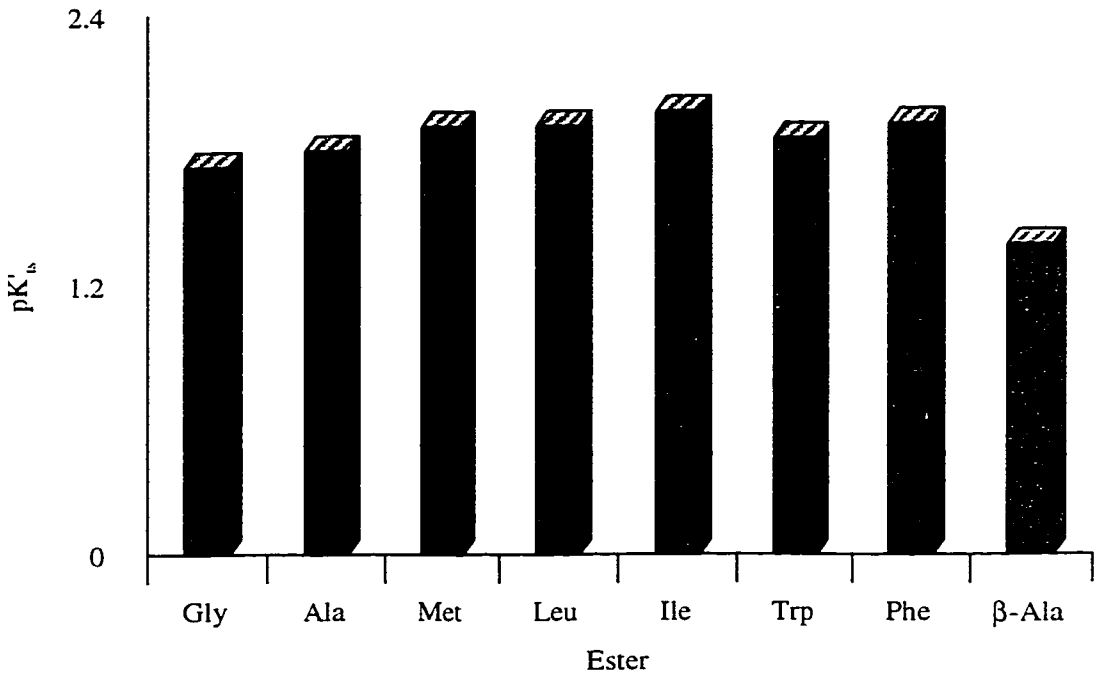

Figure 2.20 pK'_{ts} values for ternary transition state complexes.

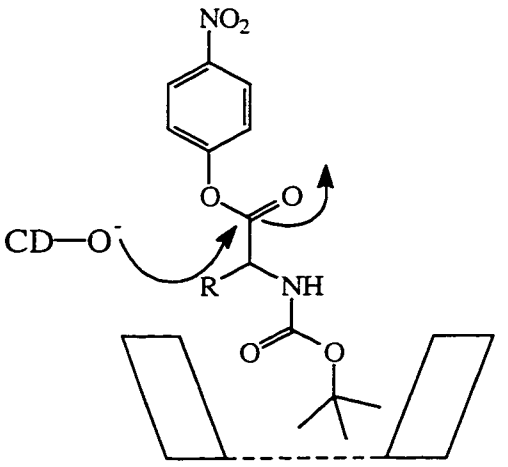

12

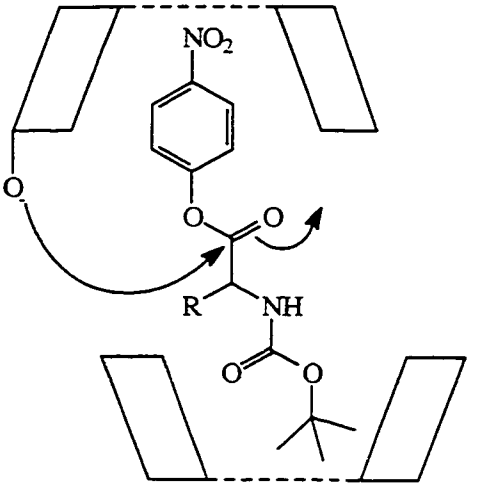

13

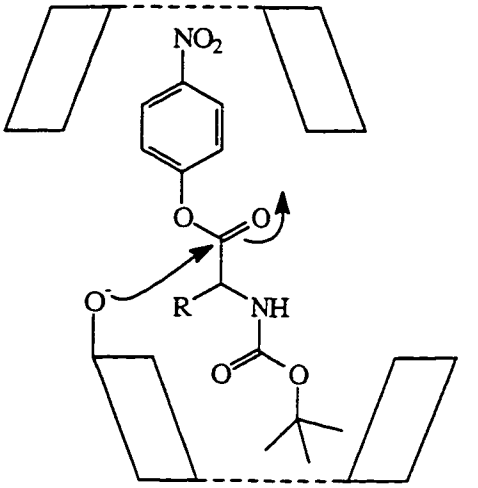

14

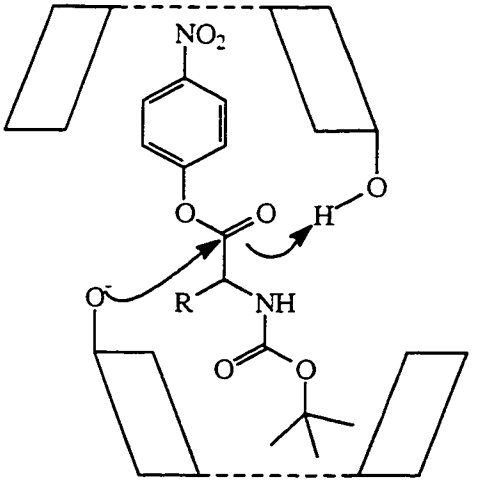

15

2.3 Structure-Activity Analysis for Ester Cleavage by γ-CD

The rates of cleavage of the BOC-Esters, and most of the CBZ-Esters by γ-CD conform to saturation kinetics as shown in Figures 2.21 and 2.22. However, for the esters of CBZ-β-Ala and CBZ-Gly-Gly, the cleavage rates are enhanced at low $[CD]_o$, but then retarded at higher $[CD]_o$ (Figure 2.23). The retardation is attributed to the formation of non-productive 1:2 (ester:CD), $S.CD_2$, complexes at higher $[CD]_o$ (2.9), in addition to reactions (2.1) and (2.2), and the kinetic behaviour is described by equation (2.10). The kinetic parameters obtained from fitting are collected in Table 2.3, along with the calculated constants.

$$S.CD + CD \underset{}{\overset{K_{s2}}{\rightleftharpoons}} S.CD_2 \qquad (2.9)$$

$$k_{obs} = \frac{k_u K_s K_{s2} + k_c K_{s2}[CD]_o}{K_s K_{s2} + K_{s2}[CD]_o + [CD]_o^2} \qquad (2.10)$$

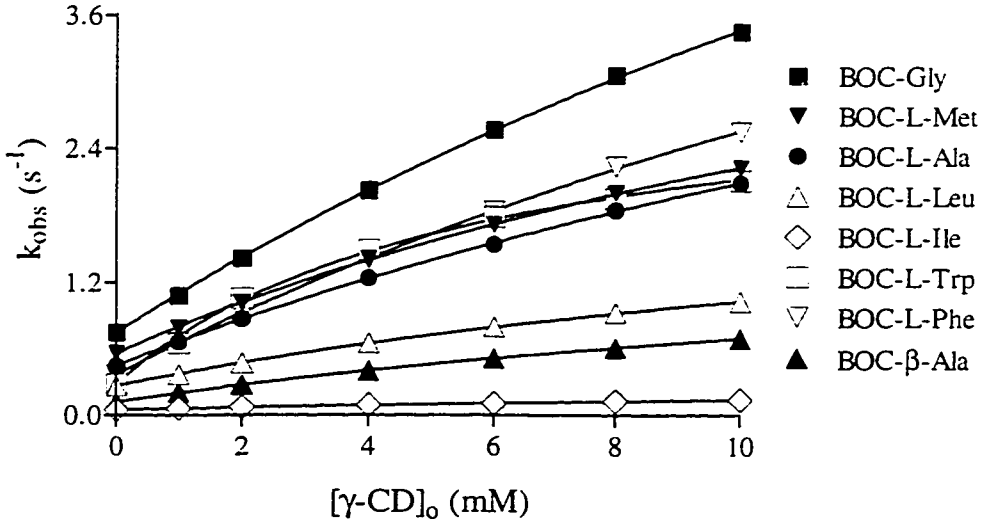

Figure 2.21 Plots of k_{obs} vs $[\gamma\text{-CD}]_o$ for cleavage of BOC-Esters.

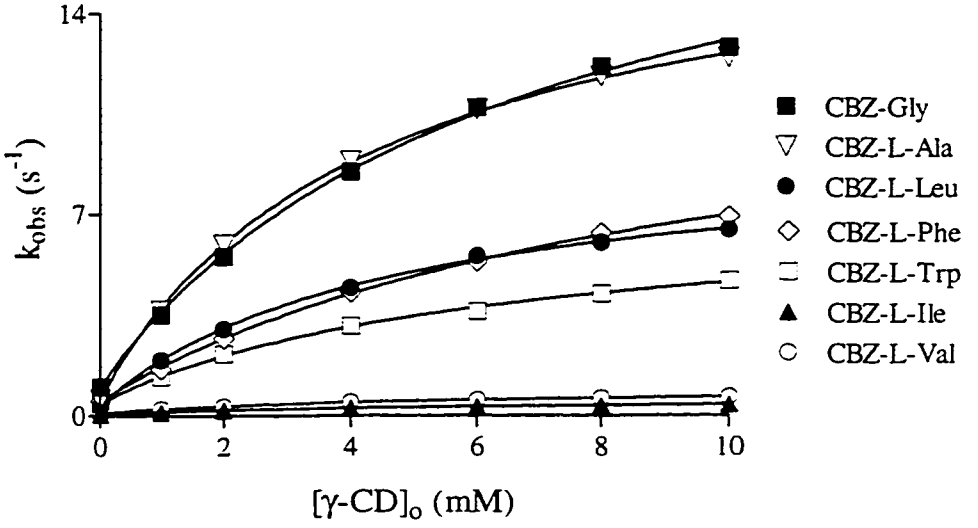

Figure 2.22 Plots of k_{obs} vs $[\gamma\text{-CD}]_o$ for cleavage of CBZ-Esters.

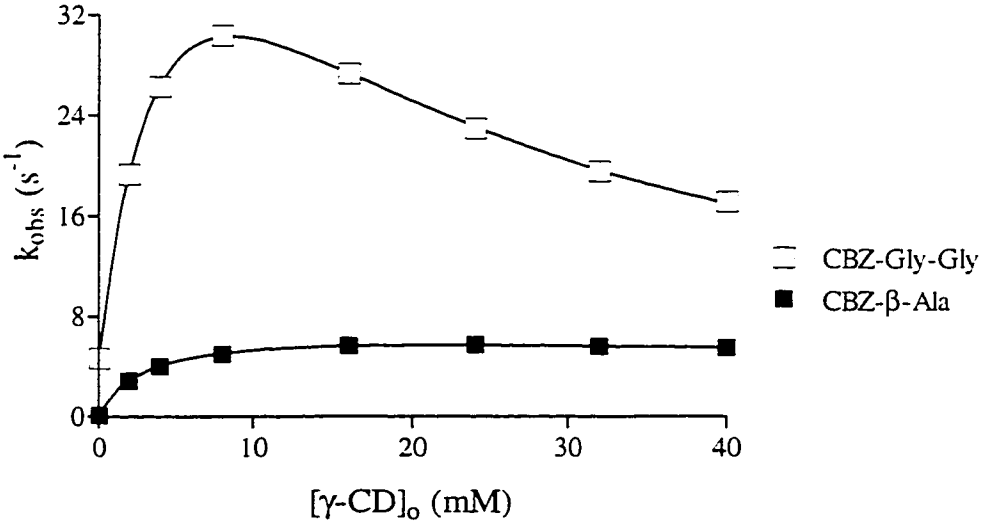

Figure 2.23 Plots of k_{obs} vs $[\gamma\text{-CD}]_o$ indicating formation of non-productive $S.CD_2$ complexes.

Table 2.3 Constants for Cleavage of Esters by γ-CD.[a]						
Ester	K_s mM	k_c s^{-1}	k_c/k_u	k_2 $M^{-1}s^{-1}$	K_{ts} mM	K_{s2} mM
BOC-Esters with γ-CD						
Gly	29.9 ± 2.2	11.5 ± 0.6	15.5	385	1.93	
L-Ala	26.4 ± 1.4	6.42 ± 0.25	14.4	243	1.84	
L-Met	19.0 ± 0.8	5.39 ± 0.15	9.63	284	1.97	
L-Leu	19.7 ± 1.5	2.53 ± 0.12	9.48	128	2.08	
L-Ile	32.9 ± 4.8	0.443 ± 0.046	9.03	13.5	3.64	
L-Trp[b]	5.62 ± 0.52	3.15 ± 0.13	11.1	561	0.504	
L-Phe[c]	26.4 ± 1.5	8.34 ± 0.34	22.8	316	1.16	
β-Ala	21.0 ± 1.3	1.89 ± 0.08	15.8	90.0	1.33	
CBZ-Esters with γ-CD						
Gly	6.64 ± 0.52	21.0 ± 0.8	20.6	3160	0.323	
L-Ala	4.43 ± 0.18	17.9 ± 0.3	30.4	4040	0.146	
L-Leu	4.64 ± 0.25	9.34 ± 0.21	26.3	2010	0.177	
L-Val	5.16 ± 0.18	0.958 ± 0.014	11.0	186	0.471	
L-Ile	5.93 ± 0.42	0.586 ± 0.018	9.78	98.8	0.606	
L-Trp[b]	6.16 ± 0.57	7.21 ± 0.31	16.5	1170	0.373	
L-Phe[c]	9.38 ± 0.57	13.0 ± 0.4	25.6	1390	0.366	
β-Ala	3.22 ± 0.11	7.33 ± 0.10	56.2	2270	0.0573	159 ± 13
Gly-Gly	6.20 ± 0.19	67.6 ± 1.2	14.4	10900	0.430	13.9 ± 0.4

[a] At 25 °C, in 0.2 M phosphate buffer, pH 11.6 containing 0.1%, [b] 5%, and [c] 10% acetonitrile. $k_2 = k_c/K_s$, $K_{ts} = k_u K_s/k_c$. k_u values are given in Table 2.1.

The accelerations, k_c/k_u, for cleavage of the BOC-Esters by γ-CD are practically the same, and this is because the K_s and K_{ts} values (or pK_s and pK_{ts} values; Figure 2.26), hardly vary. The accelerations for cleavage of the CBZ-Esters vary a bit more, primarily due to differences in transition state binding, since substrate binding for these esters is essentially the same (Figure 2.27). Overall, the largest acceleration is achieved with CBZ-β-Ala as a result of significantly stronger transition state binding.

The BOC-Esters are considerably less reactive than the CBZ-Esters with γ-CD as indicated by the lower k_2 values (Table 2.3). In fact, the CBZ-Esters appear to be most reactive with γ-CD, followed closely by β-CD. However, the BOC-Esters are slightly more reactive with γ-CD than they are with α-CD, and significantly less reactive than with β-CD. The plot of log k_2 versus log k_u (Figure 2.24) shows that the reactivities of the BOC-Esters with γ-CD are in most cases about the same. BOC-β-Ala, BOC-Phe, and BOC-Trp appear to be more reactive as a result of stronger transition state binding (Figure 2.26). The reactivities of the CBZ-Esters with γ-CD are also quite similar to each other (Figure 2.25), with the exception of CBZ-Ala, CBZ-Leu, and CBZ-β-Ala which are more reactive.

In general, the K_s values for the BOC-Esters are 3 - 10 times higher than those for the CBZ-Esters indicating that they bind much weaker to γ-CD. Also, the K_s values (or pK_s values; Figures 2.26 and 2.27), for both series of esters are quite constant. A K_s value of 35.6 mM was obtained in previous work for the binding of *p*NPA to γ-CD,[40] which is fairly comparable to the K_s values obtained with the current BOC-Esters. These facts seem to suggest that the BOC-Esters generally bind to γ-CD by the *p*NP group while the CBZ-Esters bind by the CBZ-group. The K_s value for BOC-Trp is considerably lower than those for the

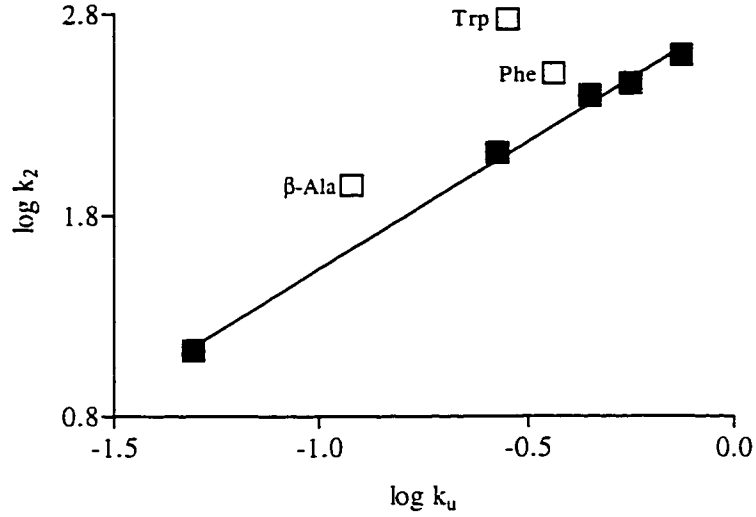

Figure 2.24 Plot of log k_2 vs log k_u for BOC-Esters with γ-CD. Linear regression analysis done with ■ only. (Slope = 1.25 ± 0.05; r = 0.998)

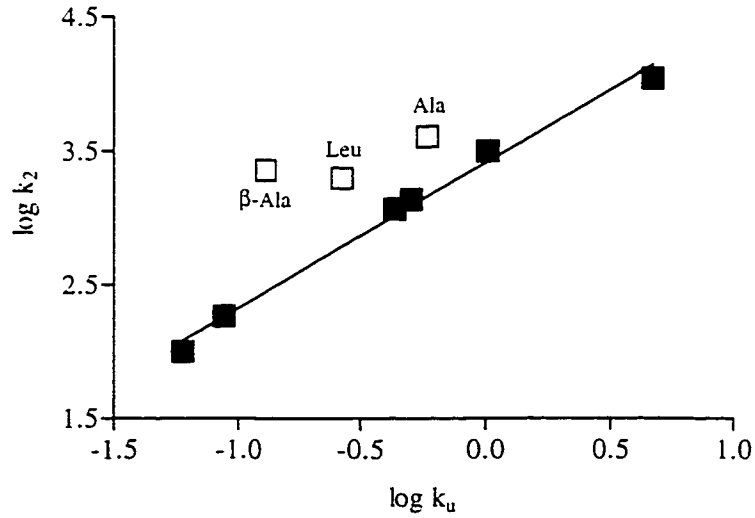

Figure 2.25 Plot of log k_2 vs log k_u for CBZ-Esters with γ-CD Linear regression analysis done with ■ only. (Slope = 1.09 ± 0.05; r = 0.995)

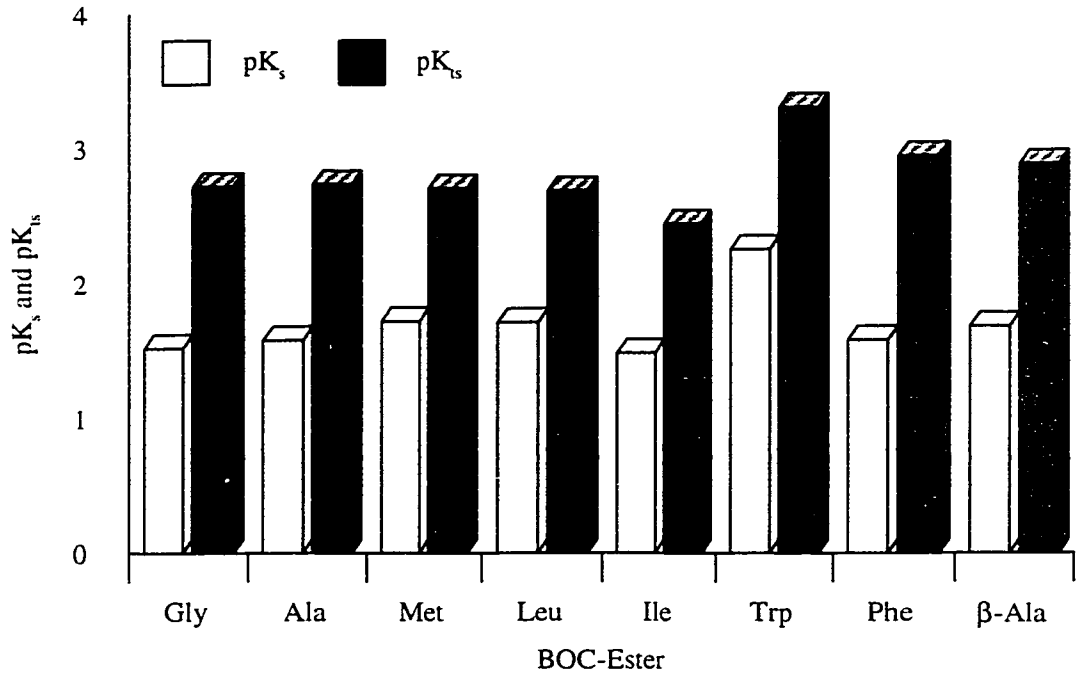

Figure 2.26 pK_s and pK_{ts} values for BOC-Esters with γ-CD.

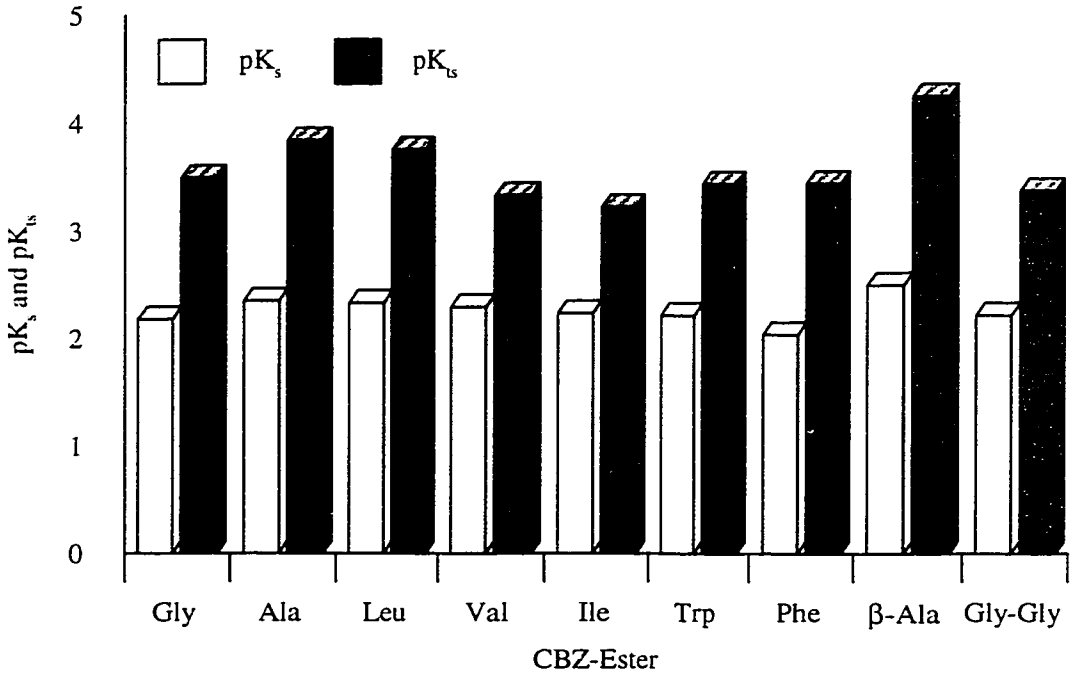

Figure 2.27 pK_s and pK_{ts} values for CBZ-Esters with γ-CD.

other BOC-Esters which suggests that this ester binds to γ-CD by its indolyl group. It is also possible that CBZ-Trp binds to γ-CD by its indolyl ring since the K_s value is within the accuracy of that for BOC-Trp. Induced c.d. spectra of weak intensity similar to that seen for *p*NPA with γ-CD were obtained for BOC-Gly and BOC-β-Ala as shown in Figure 2.28, supporting the notion that the BOC-Esters bind to γ-CD by the *p*NP group. However, the induced c.d. spectrum expected for strong binding of the *p*NP group to γ-CD was seen for CBZ-β-Ala (Figure 2.29). Moreover, the inherent c.d. peak for CBZ-L-Ala is quenched by γ-CD and induced peaks appear in the wavelength bands corresponding to inclusion of the *p*NP group (Figure 2.30). These results seem to indicate that the CBZ-Esters bind by the *p*NP group instead of the CBZ-group. Thus, the CBZ-group may actually improve binding of the *p*NP group through either a steric and/or conformational effect. The induced c.d. spectrum for CBZ-Gly is a bit more complicated (Figure 2.29), but may be indication that inclusion of the CBZ-group and inclusion of the *p*NP group are competitive modes of binding.

The K_{ts} values determined for the BOC-Esters are also appreciably higher than those obtained with the CBZ-Esters showing that transition state binding to γ-CD is much weaker. In general, the K_{ts} values for the two series of esters are fairly constant, which is reflected in the bar graphs of pK_{ts} values (Figures 2.26 and 2.27). The K_{ts} values for the BOC-Esters are close to the literature value for *p*NPA which is 2.4 mM,[40] indicating that the BOC-Esters bind by the *p*NP group and therefore, the CBZ-Esters most likely bind by the CBZ-group in the transition state. As seen in Figure 2.26, the pK_{ts} value for BOC-Trp is conspicuously higher than those for the other BOC-Esters suggesting that this ester binds by its indolyl ring in the transition state, and this may also be the case for CBZ-Trp. The pK_{ts} values for CBZ-Ala,

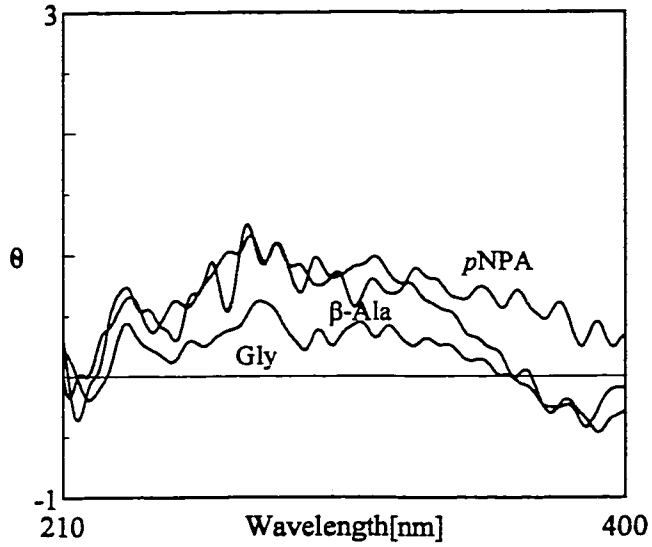

Figure 2.28 Induced c.d. spectra of *p*NPA with 50 mM γ-CD, and BOC-Gly and BOC-β-Ala with 30 mM γ-CD.

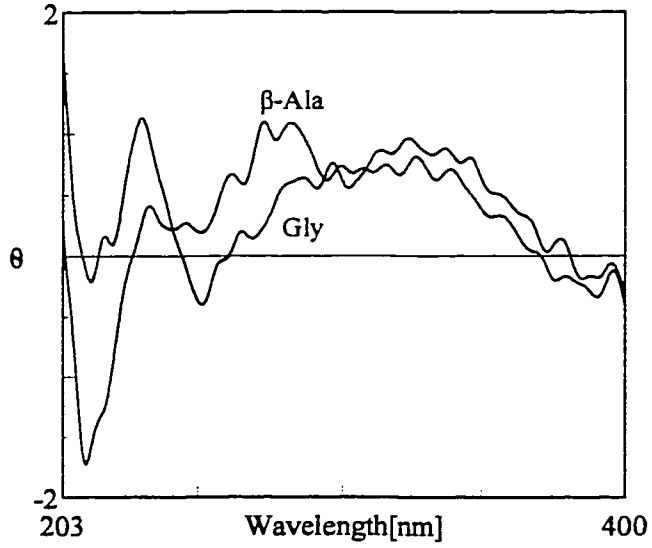

Figure 2.29 Induced c.d. spectra of CBZ-Gly and CBZ-β-Ala with 10 mM and 3 mM γ-CD respectively.

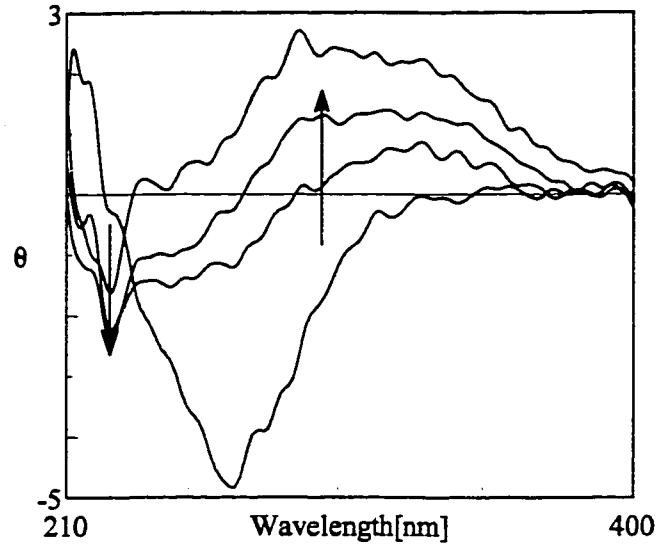

Figure 2.30 Effect of 0, 5, 10, and 15 mM γ-CD on c.d. spectrum of CBZ-L-Ala. Arrows indicate effect of increasing $[CD]_o$.

CBZ-Leu, and CBZ-β-Ala are also noticeably higher than those for the other CBZ-esters (Figure 2.27). Nevertheless, the transition state structures for these three esters are probably very similar to those of the other CBZ-Esters, but subtle differences in steric and conformational effects result in improved transition state binding.

For CBZ-β-Ala and CBZ-Gly-Gly, non-productive 1:2 (ester:CD) complexes are evident at higher $[CD]_o$ which result in retardation. This behaviour can be explained in terms of relative Gibbs free energies. By examining the Gibbs free energy diagram (Figure 2.19), one can see that the formation of a stable $S.CD_2$ complex can cause the energy required for the k'_c process to become much larger than that required for the k_c process which results in

retardation. The non-productive ($S.CD_2$) complexes formed with γ-CD are favoured by the length of the esters, the presence of phenyl rings at the two extreme ends of the esters, and the size of the CD cavity. Assuming that a second CD molecule binds weakly to CBZ-Gly but goes undetected, then the binding of the second CD molecule improves with the length of the esters along the series: CBZ-Gly < CBZ-β-Ala < CBZ-Gly-Gly.

2.4 Effects of Cyclodextrins on Intramolecular Ester Cleavage

More than forty years ago, it was discovered that the hydrolysis of CBZ-L-Asn methyl ester (**20**) led primarily to the formation of the imide, CBZ-L-aminosuccinimide (**22**) instead of the corresponding acid, CBZ-L-Asn (**21**) (Figure 2.31).[66] About 90% of the reaction involved formation of the imide (**22**). The mechanism is believed to involve intramolecular nucleophilic attack by the nitrogen of the ionized internal amide group on the ester function. The methyl ester of CBZ-L-Gln, which differs from its CBZ-L-Asn counterpart by the presence of an additional methylene group in the amino acid side chain, also gives the imide, CBZ-D,L-α-aminoglutarimide, in basic solution.

Several other intramolecular reactions involving nucleophilic attack by internal amide groups have been reported.[34,59-61] However, amides are not known for their nucleophilicity and the reaction of acetamide with *p*NPA in basic solution, an intermolecular analog for imide formation, showed no rate increase over the background reaction.[60] A similar result was obtained for the reaction of acetamide with CBZ-Gly in this work.

The effects of α-CD, β-CD, and γ-CD on the cleavage of the *p*-nitrophenyl esters of BOC-L-Asn, CBZ-L-Asn, BOC-L-Gln and CBZ-L-Gln in basic media were studied in this work and the kinetic parameters are collected in Table 2.4. Modest rate enhancements were observed for cleavage of all four esters with α-CD and γ-CD, and for BOC-Gln and CBZ-Gln with β-CD. The rate data in most cases conform to simple saturation-type behaviour, equation (2.3), except for CBZ-Gln with α-CD, where the dependence of k_{obs} on $[CD]_o$ is linear, equation (2.5). In the cases of BOC- and CBZ-Asn with β-CD, the cleavage process is initially retarded at lower $[CD]_o$, but then enhanced at higher $[CD]_o$. However, the kinetics

are well described by equation (2.7). Plots of k_{obs} versus $[CD]_o$ for cleavage of BOC-Asn and CBZ-Asn in the presence of α-CD, β-CD and γ-CD are shown in Figures 2.32 and 2.33.

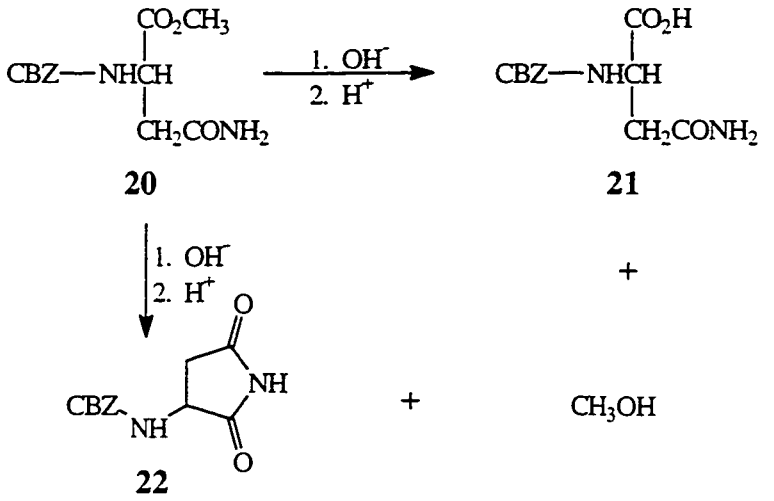

Figure 2.31 Cleavage of CBZ-L-Asn methyl ester.

The accelerations, k_c/k_u, for the cleavage of BOC–Asn, CBZ-Asn, and BOC-Gln are virtually the same and this is because the K_s values for the three esters are practically the same, as well as the K_{ts} values (Table 2.4). For CBZ-Gln with α-CD, k_c/k_u and K_s values could not be determined since saturation kinetics were not observed. Nevertheless, the K_{ts} value is essentially the same as those obtained for the other three esters. The K_{ts} values for these four esters are higher than those for other BOC- and CBZ-Esters with amino acid side chains of similar size, such as BOC- and CBZ-Leu (Table 2.1), which suggests that the transition state structures are less stable and may be different. Perhaps, the rate enhancements observed for these four esters with α-CD are due to a conformational effect (i.e., non-covalent catalysis) which promote formation of the respective imides.

Table 2.4 Kinetic parameters for intramolecular ester cleavage.[a]

L-Ester	K_s mM	k_c s^{-1}	k_c/k_u	k_2 $M^{-1}s^{-1}$	K_{ts} mM	k_{c2} $M^{-1}s^{-1}$	K'_{ts} mM
α-CD							
BOC-Asn[b]	31.8 ± 4.8	10.8 ± 0.6	2.32	340	13.7		
BOC-Gln	47.1 ± 3.0	6.38 ± 0.17	3.07	136	15.4		
CBZ-Asn[b]	43.7 ± 8.7	15.5 ± 1.4	2.65	355	16.5		
CBZ-Gln				147	17.8		
β-CD							
BOC-Asn[b]	0.747 ± 0.050	2.84 ± 0.04	0.610	3800	1.22	85.2 ± 5.1	33.3
BOC-Gln	5.59 ± 0.60	11.4 ± 0.5	5.46	2030	1.02		
CBZ-Asn[b]	2.22 ± 0.44	5.01 ± 0.07	0.859	2260	2.59	122 ± 10	41.9
CBZ-Gln	10.0 ± 0.4	15.7 ± 0.3	5.99	1570	1.68		
γ-CD							
BOC-Asn[b]	15.5 ± 2.9	5.92 ± 0.13	1.27	382	12.2		
BOC-Gln	47.9 ± 6.7	19.9 ± 1.9	9.57	415	5.01		
CBZ-Asn[b]	4.26 ± 0.52	8.08 ± 0.08	1.38	1900	3.08		
CBZ-Gln	5.09 ± 0.26	25.3 ± 0.5	9.66	4970	0.527		

[a] At 25 °C, in 0.2 M phosphate buffer, pH 11.6, 0.1% acetonitrile. [b] Done in 0.2 M carbonate buffer, pH 10.6, 0.1% acetonitrile. The k_u values for BOC-Asn, BOC-Gln, CBZ-Asn and CBZ-Gln are 4.65, 2.08, 5.84, and 2.62 s^{-1} respectively.

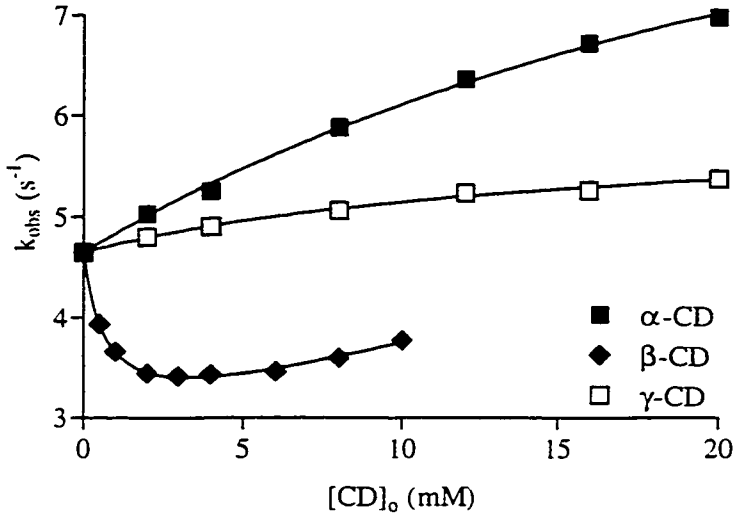

Figure 2.32 Effects of α-, β-, and γ-CDs on the cleavage of BOC-L-Asn *p*NP ester.

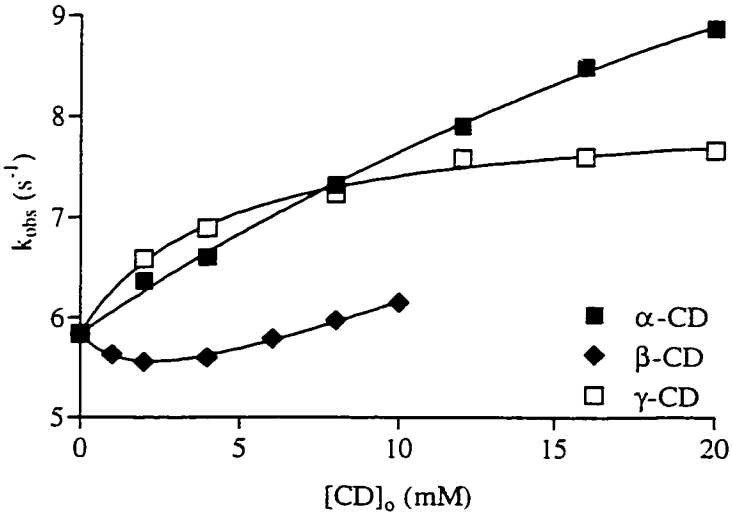

Figure 2.33 Effects of α-, β-, and γ-CDs on the cleavage of CBZ-L-Asn *p*NP ester.

As mentioned earlier, cleavage of BOC- and CBZ-Asn is retarded at lower $[\beta\text{-CD}]_o$ ($k_c/k_u < 1$), and accelerated at higher $[\beta\text{-CD}]_o$. The initial retardation in each case is due to the fact that substrate binding is significantly stronger than transition state binding ($K_s << K_{ts}$). Apparently, these esters are buried deep inside the β-CD cavities in non-productive modes in the initial S.CD complex, and have to partially dissociate to facilitate intramolecular amide attack and consequent imide formation. The rate enhancements observed at higher $[\beta\text{-CD}]_o$ are likely due to nucleophilic attack by a second β-CD molecule on the non-productive S.CD complexes. Of course, as discussed earlier, there is a possibility that productive ternary $S.CD_2$ complexes are formed at higher $[\beta\text{-CD}]_o$ which are responsible for the rate enhancements observed. Incidentally, the K'_{ts} values for the ternary transition state complexes, $TS.CD_2$, of these two esters with β-CD are practically the same suggesting that the transition state structures are very similar.

For BOC- and CBZ-Gln, the cleavage rates are enhanced by β-CD ($k_c/k_u > 1$) because substrate binding is weaker than transition state binding ($K_s > K_{ts}$). The K_s values for BOC- and CBZ-Gln are noticeably higher than those for the corresponding BOC- and CBZ-Asn esters. However, the K_{ts} value for BOC-Gln is comparable to that for BOC-Asn indicating that their transition state structures are similar, and likewise, the K_{ts} value for CBZ-Gln is comparable to that for CBZ-Asn. In fact the transition state structures for all four esters may be the same since the K_{ts} values do not differ significantly. Moreover, since the K_{ts} values for these esters are about 3 to 6-fold higher than those for other esters containing amino acid side chains of similar size (Table 2.2), it is possible that non-covalent transition state intermediates are formed for these four esters with β-CD.

The accelerations achieved for the cleavage of BOC- and CBZ-Gln in the presence of γ-CD are much better than those obtained with BOC- and CBZ-Asn, even though the accelerations are in general pretty modest. Compared to BOC-Gln, the smaller acceleration seen with BOC-Asn results from a combination of stronger substrate binding and weaker transition state binding. The smaller acceleration seen with CBZ-Asn relative to CBZ-Gln is due primarily to weaker transition state binding, since the strength of substrate binding for these two esters to γ-CD is basically the same. The K_{ts} values for BOC- and CBZ-Gln are comparable to those for most of the BOC- and CBZ-Esters (Table 2.3) suggesting that the transition state structures are similar, and may involve covalent bond formation (i.e., covalent catalysis). The K_{ts} values for BOC-Asn and CBZ-Asn are higher than those for BOC-Gln and CBZ-Gln, as well as those for the other BOC- and CBZ-Esters, suggesting that the transition state structures may be different and do not involve covalent bond formation.

2.5 Enantioselective Cleavage by Cyclodextrins

Cyclodextrins are inherently chiral due to the asymmetry of their glucopyranose units, and they exhibit enantioselectivity in a number of reactions.[1,5,62-65] Enantioselectivity is observed for the cleavage of carboxylic esters,[1,5,62,63,65] carbonates,[62,63] organophosphates,[1,5] amino acid esters,[1,64] and so on. However, the enantioselectivity in most cases is only modest. So far, the largest enantioselectivity factor (greater than 60) has been observed for the cleavage of a pair of ferrocene based *p*-nitrophenyl esters by β-CD.[65]

In this work, the cleavage of a few pairs of enantiomers has been studied and most of the kinetic parameters for the L-Esters have already been given. Kinetic parameters for the D-Esters, and a pair of N-hydroxysuccinimide esters (HSE) of BOC-L-Pro and BOC-D-Pro are given in Table 2.5. The kinetics in most cases are consistent with simple saturation-type behaviour. However, there were cases with α-CD where the dependence of k_{obs} on $[CD]_o$ was linear.

The enantioselectivity is expressed in terms of the ratios (k_2^L/k_2^D), $(k_c/k_u)^L/(k_c/k_u)^D$, and in some cases, k_{c2}^L/k_{c2}^D. The first two ratios convey the enantioselectivity at non-saturating and saturating $[CD]_o$ respectively, while the last term expresses the enantioselectivity exhibited by a second CD molecule reacting with an initial S.CD complex. From the ratios in Table 2.6, it can be seen that for each pair of enantiomeric esters, the L-Ester in most instances is cleaved faster than the D-Ester in the presence of cyclodextrins. The bar graphs of pK_s and pK_{ts} values (Figures 2.34, 2.35, and 2.36), show that the origin of this enantioselectivity comes almost solely from stronger transition state binding of the L-Esters, although there are instances where differences in the strengths of substrate binding between

Table 2.5 Kinetic Parameters for D-Esters.[a]					
Ester	K_s mM	k_c s^{-1}	k_c/k_u	k_2 $M^{-1}s^{-1}$	K_{ts} mM
α-CD					
BOC-D-Gln	51.9 ± 7.5	5.53 ± 0.32	2.65	107	19.6
BOC-D-Phe[b]	240 ± 27	3.36 ± 0.30	9.27	14.0	25.9
CBZ-D-Phe[b]				10.1	50.8
BOC-L-Pro HSE				162	9.63
BOC-D-Pro HSE				160	9.73
β-CD					
BOC-D-Gln	6.80 ± 0.96	5.25 ± 0.22	2.51	771	2.71
BOC-D-Phe[b]	2.21 ± 0.05	5.25 ± 0.04	14.5	2380	0.152
CBZ-D-Phe[b]	9.03 ± 0.30	4.80 ± 0.08	9.38	532	0.962
BOC-L-Pro HSE	0.644 ± 0.045	64.2 ± 0.6	41.2	99700	0.0156
BOC-D-Pro HSE	1.24 ± 0.14	20.1 ± 0.5	12.9	16100	0.0967
γ-CD					
BOC-D-Gln	70.5 ± 8.7	7.69 ± 0.57	3.68	109	19.2
BOC-D-Phe[b]	30.2 ± 1.3	2.78 ± 0.08	7.66	92.1	3.94
CBZ-D-Phe[b]	13.9 ± 1.7	3.91 ± 0.27	7.64	281	1.82
BOC-L-Pro HSE	13.5 ± 0.8	23.3 ± 0.8	15.0	1730	0.904
BOC-D-Pro HSE	15.7 ± 1.28	16.9 ± 0.9	10.9	1080	1.44

[a] At 25 °C, in 0.2 M phosphate buffer, pH 11.6, 0.1% and [b] 10% acetonitrile. k_u values can be found in the Appendix. HSE = Hydroxysuccinimide esters.

Table 2.6 Kinetic ratios for (L/D)-enantioselectivity.			
Enantiomers	k_2^L/k_2^D	$(k_c/k_u)^L/(k_c/k_u)^D$	k_{c2}^L/k_{c2}^D
α-CD			
BOC-Gln	1.27	1.14	
BOC-Phe	1.53	0.970	
CBZ-Phe	1.37		
BOC-Pro HSE	1.01		
β-CD			
BOC-Gln	2.63	2.18	
BOC-Phe	0.861	1.00	v. large
CBZ-Phe	1.51	2.16	
BOC-Pro HSE	6.19	3.19	
γ-CD			
BOC-Gln	3.81	2.60	
BOC-Phe	3.43	2.98	
CBZ-Phe	4.93	3.34	
BOC-Pro HSE	1.60	1.38	

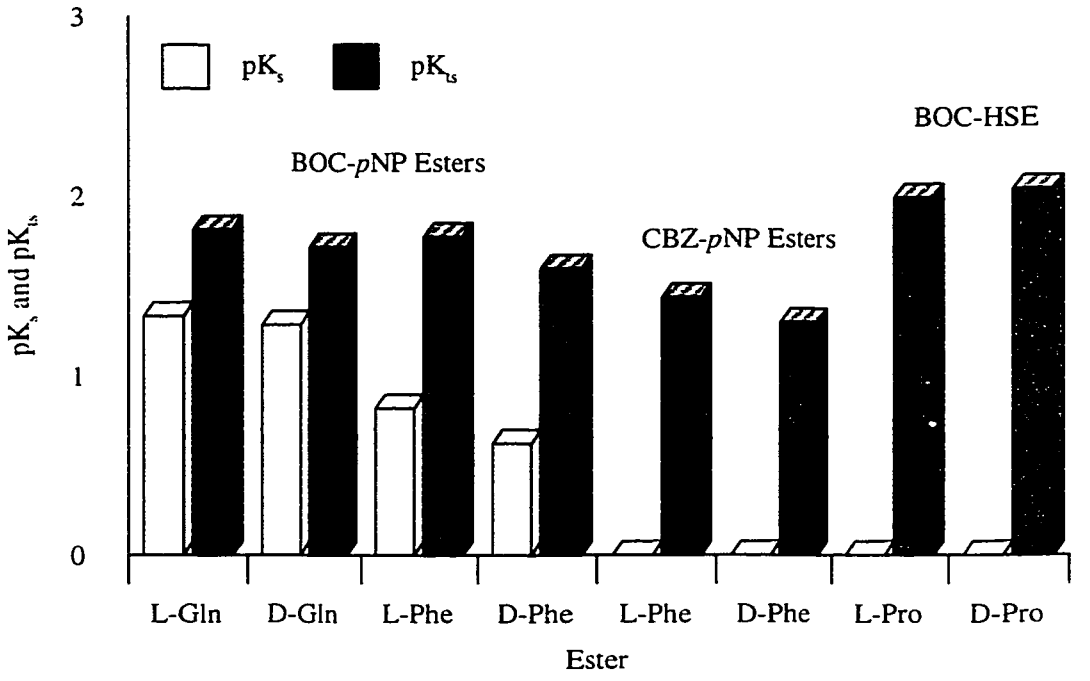

Figure 2.34 pK_s and pK_{ts} values for L- and D-Esters with α-CD.

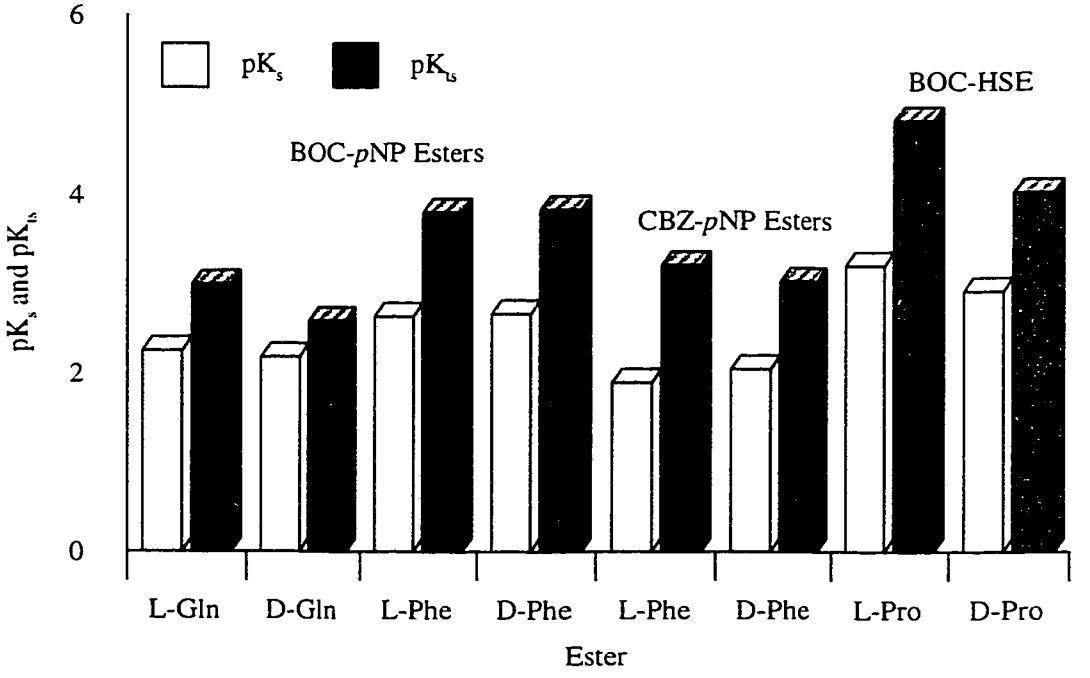

Figure 2.35 pK_s and pK_{ts} values for L- and D-Esters with β-CD.

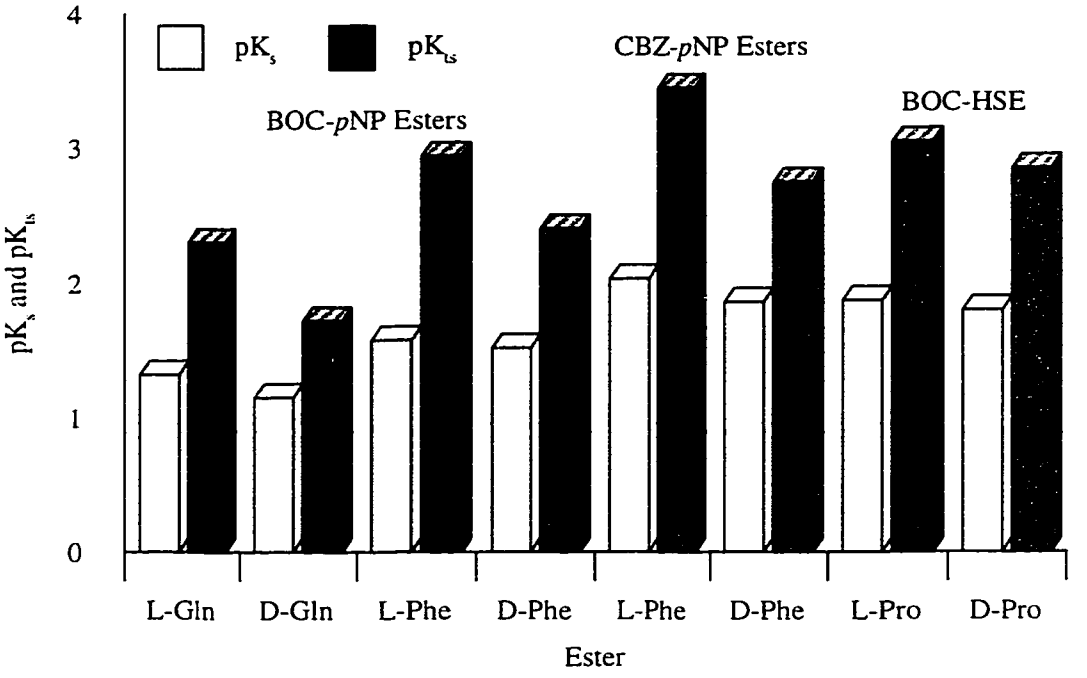

Figure 2.36 pK$_s$ and pK$_{ts}$ values for L- and D-Esters with γ-CD.

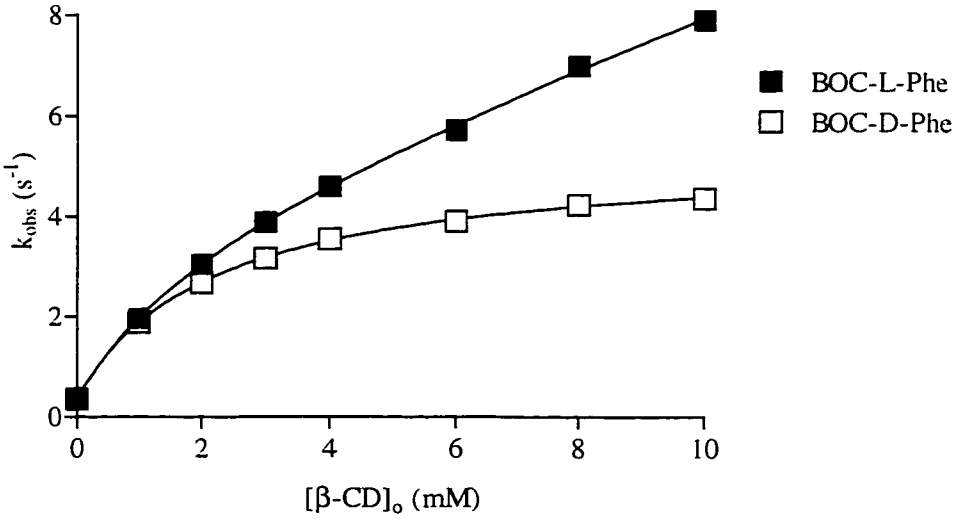

Figure 2.37 Plots of k$_{obs}$ vs [β-CD]$_o$ for BOC-Phe enantiomers.

pairs of enantiomers influence the enantioselectivity. For cleavage of the *p*-nitrophenyl ester derivatives given in Table 2.6, the highest enantioselectivity ratios are seen with γ-CD, followed by β-CD. However, for the pair of N-hydroxysuccinimide esters, the highest ratios are seen with β-CD, while no enantioselectivity is observed with α-CD.

Figure 2.37 contains plots of k_{obs} versus $[\beta\text{-CD}]_o$ for the cleavage of BOC-Phe enantiomers. At low $[\beta\text{-CD}]_o$, there is virtually no difference between the two curves which explains why the ratios k_2^L/k_2^D and $(k_c/k_u)^L/(k_c/k_u)^D$ are near 1. This is because the pK_s values for both the L- and D-Esters, as well as the pK_{ts} values (Figure 2.35) are basically equal. However, at higher $[\beta\text{-CD}]_o$, the curve for the L-Ester becomes significantly higher than that for the D-Ester, indicating that the k_{c2} process for the L-Ester is much more efficient than that for the D-Ester. In fact, no evidence was found for the involvement of a second CD in the cleavage of the D-Ester.

3. CONCLUSIONS

Cleavage of the BOC- and CBZ-Esters in basic aqueous solution by cyclodextrins generally occurs through 1:1 (ester:CD) complexes. Even though complexation was not detected for cleavage of most of the CBZ-Esters by α-CD, it is possible that reaction occurs within weak 1:1 (ester:CD) complexes. A second cleavage pathway involving either reaction of a 1:1 (ester:CD) complex with a second CD molecule, or reaction within a weak 1:2 (ester:CD) complex is apparent for cleavage of the BOC-Esters by β-CD. For cleavage of the esters of CBZ-β-Ala and CBZ-Gly-Gly by γ-CD, an additional process involving the formation of non-productive 1:2 (ester:CD) complexes is evident.

Generally speaking, the reactivity of the BOC-Esters under non-saturating $[CD]_o$ increases as follows: α-CD < γ-CD << β-CD. For the CBZ-Esters, the reactivity generally increases along the series: α-CD << β-CD < γ-CD. These trends in reactivity parallel those in the strength of transition state binding. However, the increasing strength of transition state binding does not result in substantially better accelerations since the strength of substrate binding increases almost by the same extent.

In general, substrate binding for both the BOC- and CBZ-Esters in the 1:1 (ester:CD) complexes seems to involve inclusion of the *p*NP group. However, substrate binding for the BOC-Esters to β-CD appears to occur by the BOC-group, while binding of the CBZ-Esters to γ-CD seems to involve inclusion of either the CBZ-group, or the *p*NP group. BOC-Trp appears to bind to β-CD and γ-CD by the indolyl ring, and this may also be the situation for CBZ-Trp.

Transition state binding for the 1:1 cleavage process seems to generally involve inclusion of the *p*NP group except for the BOC-Esters with β-CD, where the BOC-group likely resides inside the β-CD cavity, and the CBZ-Esters with γ-CD where binding in the transition state may involve inclusion of the CBZ-group. For BOC- and CBZ-Trp, transition state binding to β-CD and γ-CD most likely involves inclusion of the indolyl group.

The rates of cleavage of BOC-Asn, CBZ-Asn, BOC-Gln, and CBZ-Gln, which undergo intramolecular nucleophilic attack by their internal amide groups in basic solution, are generally enhanced by cyclodextrins through the usual 1:1 (ester:CD) complexes. However, cleavage of BOC- and CBZ-Asn in the presence of β-CD is retarded at low $[CD]_o$ due to the formation of non-productive 1:1 (ester:CD) complexes, and then accelerated at higher $[CD]_o$ as a result of either nucleophilic attack by free CD anions on the non-productive ester/CD complexes, or reaction within weak productive 1:2 (ester:CD) complex.

In general, the rates of cleavage of esters containing L-amino acids are faster than their D-analogues in the presence of cyclodextrins. The faster cleavage rates observed for the L-enantiomers are due primarily to better stabilization of the transition states by cyclodextrins.

4. EXPERIMENTAL

4.1 Materials

The *p*-nitrophenyl esters of N-*tert*-butyloxycarbonyl and N-benzyloxycarbonyl amino acids, as well as the pair of N-hydroxysuccinimide esters of N-*tert*-butyloxycarbonyl proline were purchased from the Sigma Chemical Company. The cyclodextrins were purchased from the Aldrich Chemical Company and from Wacker-Chemie. Sodium phosphate (dibasic, heptahydrate), sodium bicarbonate, and all of the other reagents were obtained from the Aldrich Chemical Company. These compounds were used without further purification.

4.2 Kinetic Experiments

The kinetic experiments were carried out by 1:1 mixing in a stopped-flow apparatus connected to an Applied Photophysics SX17MV spectrophotometer at 25.0 ± 0.1 °C. All solutions were prepared at twice the desired concentrations. CD solutions were prepared in 0.4 M phosphate buffer, pH 11.6. For experiments with BOC- and CBZ-Asn, CD solutions were prepared in 0.4 M carbonate buffer, pH 10.6, since these reactions are too fast at pH 11.6 to be accurately monitored. The pH of the buffers were measured with an Accumet Model 25 pH/ion meter, and any required adjustments to the pH were done with either concentrated NaOH or HCl. High buffer concentrations were employed to counteract the weak acidity of the secondary hydroxyl groups on the cyclodextrins. Solutions of 20 μM of the *p*-nitrophenyl esters and 200 μM of the N-hydroxysuccinimide esters in water were used for the experiments, which were prepared from stock solutions of 0.01 M and 0.1 M in

HPLC grade acetonitrile, respectively. The concentrations of these solutions were halved after mixing in the stopped-flow apparatus. Additional acetonitrile was needed to dissolve the Trp and Phe esters in water so that the acetonitrile content was 5% and 10%, respectively, after mixing.

The kinetics of the cleavage of the *p*-nitrophenyl esters were followed by monitoring the appearance of the *p*-nitrophenolate anion at 405 nm. For the N-hydroxysuccinimide esters, the kinetics were followed by monitoring the increase in absorbance at 231 nm. Pseudo first-order kinetics were established by using $[ester]_o << [CD]_o$. The pseudo first-order rate constant, k_{obs}, for conversion of substrate into product (4.1), is given by (4.2), where $[S]_o$ is the initial substrate concentration and [S] is the substrate concentration at any time t. Applying the mass balance relationships (4.3) and (4.4) leads to equation (4.5) where $[P]_\infty$ is the final concentration of product and [P] is the product concentration at any time t. Then making use of the Beer-Lambert law, which basically states that the concentration of a chromophore is directly proportional to its absorbance, A, gives equation (4.6).

$$S \xrightarrow{k_{obs}} P \tag{4.1}$$

$$k_{obs} = (1/t) \ln ([S]_o/[S]) \tag{4.2}$$

$$[S]_o = [P]_\infty \tag{4.3}$$

$$[S] = [S]_o - [P] = [P]_\infty - [P] \tag{4.4}$$

$$k_{obs} = (1/t) \ln \frac{[P]_\infty}{([P]_\infty - [P])} \quad (4.5)$$

$$k_{obs} = (1/t) \ln \frac{(A_\infty - A_o)}{(A_\infty - A)} \quad (4.6)$$

Absorbance traces (i.e., plots of A vs t) were collected each comprising 400 points covering about 10 half-lives were collected and the k_{obs} values were estimated by analysing these traces using a non-linear least square fitting of equation (4.7), using a software program provided by the instrument manufacturer.

$$A = (A_o - A_\infty) \exp(-k_{obs}.t) + A_\infty \quad (4.7)$$

4.3 Circular Dichroism Experiments

Circular dichroism spectra were obtained using a Jasco J-710 spectropolarimeter at room temperature in the wavelength region between 200 and 400 nm. The band width, response, step resolution, scan speed, and path length of the cell were 1.0 nm, 0.25 s, 0.5 nm, 200 nm/min, and 1.0 cm respectively. Each spectrum reported is an average of 10 scans (which improves the signal to noise ratio) and was smoothed with a mathematical algorithm, using a software program provided by the manufacturer. The observed ellipticity, θ, is given in units of mdeg.

The concentration of the esters used were 100 μM in 1% acetonitrile solution prepared from a stock solution of 0.01 M in acetonitrile. CBZ-L-Ala and CBZ-β-Ala had to be dissolved in 5% acetonitrile solution in the absence of CD. However, these esters did dissolve in the 1% acetonitrile solution when cyclodextrins were added. To ensure that complex formation occurred, CD concentrations close to or greater than the dissociation constants, K_s, were used.

REFERENCES

1. M.L. Bender, M. Komiyama, *Cyclodextrin Chemistry*, Springer-Verlag, New York, **1978**

2. (a) J. Szejtli, *Cyclodextrins and their Inclusion Complexes*, Akademial Kiado, Budapest, **1988**

   (b) J. Szejtli, *Cyclodextrin Technology*, Kluwer Academic Publishers, Dordrecht, **1988**

   (c) *Proceeding of the First International Symposium on Cyclodextrins*, J. Szejtli, (Ed), D. Reidel Publishing Company, Dordrecht, **1982**

3. *Inclusion Compounds*, Vol. 3, J.L. Atwood, J.E.D. Davies, D.D. MacNicol, (Eds) Academic Press, London, **1984**

4. P.R. Sundararajan, V.S. Rao, *Carbohydr. Res.*, **1970**, *13*, 351

5. O.S. Tee, *Advances in Physical Organic Chemistry*, **1994**, *29*, 1

6. A.J. Kirby, *Angew. Chem. Int. Ed. Engl.* **1996**, *35*, 707

7. Y. Inoue, T. Okuda, Y. Miyata, R. Chujo, *Carbohydr. Res.*, **1984**, *125*, 65

8. M. Fujiki, T. Deguchi, I. Sanemasa, *Bull. Chem. Soc. Jpn.*, **1988**, *61*, 1163

9. I. Sanemasa, Y. Akamine, *Bull. Chem. Soc. Jpn.*, **1987**, *60*, 2059

10. T. Takuma, T. Deguchi, I. Sanemasa, *Bull. Chem. Soc. Jpn.*, **1991**, *64*, 480

11. T. Osajima, T. Deguchi, I. Sanemasa, *Bull. Chem. Soc. Jpn.*, **1991**, *64*, 2705

12. I. Sanemasa, T. Takuma, T. Deguchi, *Bull. Chem. Soc. Jpn.*, **1989**, *62*, 3098

13. M. Nishimura, T. Deguchi, I. Sanemasa, *Bull. Chem. Soc. Jpn.*, **1989**, *62*, 3718

14. Y. Inoue, T. Hakushi, Y. Lui, L-H. Tong, B-J. Shen, D-S. Jin, *J. Am. Chem. Soc.*, **1993**, *115*, 475

15. R.J. Bergeron, R. Rowan, *Bioorg. Chem.*, **1976**, *5*, 425

16. R.J. Bergeron, M.A. Channing, *Bioorg. Chem.*, **1976**, *5*, 437

17. R.J. Bergeron, M.A. Channing, G.J. Gibeily, D.M. Pillor, *J. Am. Chem. Soc.*, **1977**, *99*, 5146

18. J. Szejtli, Reference 3, Chapter 11

19. R.J. Bergeron, Reference 3, Chapter 12

20. R. Breslow, Reference 3, Chapter 14

21. Y. Matsui, T. Nishioka, T. Fujita, *Top. Curr. Chem.*, **1985**, *128*, 61

22. Y. Matsui, K. Mochida, *Bull. Chem. Soc. Jpn.*, **1979**, *52*, 2808

23. O.S. Tee, M.J. Boyd, *J. Chem. Soc., Perkin Trans. 2*, **1993**, 1237

24. G.C. Catena, F.V. Bright, *Anal. Chem.*, **1989**, *61*, 905

25. P.D. Ross, M.V. Rekharsky, *Biophysical Journal*, **1996**, *71*, 2144

26. P.C. Manor, W. Saenger, *J. Am. Chem. Soc.*, **1974**, *96*, 3630

27. O.S. Tee, T.A. Gadosy, J.B. Giorgi, *J. Chem. Soc., Perkin Trans. 2*, **1993**, 1705

28. O.S. Tee, A.A. Fedortchenko, P.G. Loncke, *J. Chem. Soc., Perkin Trans. 2*, **1996**, 1243

29. O.S. Tee, T.A. Gadosy, J.B. Giorgi, *Can. J. Chem.*, **1996**, *74*, 736

30. V. Rüdiger, A. Eliseev, S. Simova, H-J. Schneider, M.J. Blandamer, P.M. Cullis, A.J. Meyer, *J. Chem. Soc., Perkin Trans. 2*, **1996**, 2119

31. J.H. Park, T.H. Nah, *J. Chem. Soc., Perkin Trans. 2*, **1994**, 1359

32. J.L. Kurz, *J. Am. Chem. Soc.*, **1963**, *85*, 987

33. J.L. Kurz, *Acc. Chem. Res.*, **1972**, *5*, 1

34. W.P. Jencks, *Catalysis in Chemistry and Enzymology*, Dover Publications, Inc., New York, **1989**

35. K.J. Laidler, *Chemical Kinetics*, 3rd edn., Harper & Row, New York, **1987**

36. R. Breslow, *Acc. Chem. Res.*, **1995**, *28*, 146

37. D.W. Griffiths, M.L. Bender, *J. Am. Chem. Soc.*, **1973**, *95*, 1679

38. O.S. Tee, R.A. Donga, *J. Chem. Soc., Perkin Trans. 2*, **1996**, 2763

39. (a) R.L. VanEtten, J.F. Sebastian, G.A. Clowes, M.L. Bender, *J. Am. Chem.* Soc.. **1967**, *89*, 3242

(b) R.L. VanEtten, G.A. Clowes, J.F. Sebastian, M.L. Bender, *J. Am. Chem. Soc.*, **1967**, *89*, 3253

40. O.S. Tee, T.A. Gadosy, *J. Chem. Soc., Perkins Trans. 2*, **1994**, 2191

41. G.M. Bonora, R. Fornasier, P. Scrimin, U. Tonellato, *J. Chem. Soc., Perkin Trans. 2*, **1985**, 367

42. O.S. Tee, C. Mazza, X-x. Du, *J. Org. Chem.* **1990**, *55*, 3603

43. O.S. Tee, X-x. Du, *J. Am. Chem. Soc.*, **1992**, *114*, 620

44. T.A. Gadosy, O.S. Tee, *J. Chem. Soc., Perkin Trans. 2*, **1994**, 715

45. J.B. Giorgi, O.S. Tee, *J. Am. Chem. Soc.*, **1995**, *117*, 3633

46. A. Fersht, *Enzyme Structure and Mechanism*, 2nd edn., W.H. Freeman and Company, New York, **1985**

47. J. March, *Advanced Organic Chemistry*, 3rd edn., John Wiley & Sons, New York,

1985

48. T.W. Solomons, *Organic Chemistry*, 6th edn., John Wiley & Sons Inc., New York, **1996**

49. O.S. Tee, *Carbohydr. Res.*, **1989**, *192*, 181

50. M. Kamiya, S. Mitsuhashi, M. Makino, H. Yoshioka, *J. Phys. Chem.*, **1992**, *96*, 95

51. G. Marconi, S. Monti, B. Mayer, G. Köhler, *J. Phys. Chem.*, **1995**, *99*, 3943

52. K. Harata, H. Uedaira, *Bull. Chem. Soc. Jpn.*, **1975**, *48*, 375

53. H. Shimizu, A. Kaito, M. Hatano, *Bull. Chem. Soc. Jpn.*, **1979**, *52*, 2678

54. M. Kajtár, C. Horváth-Toró, É. Kuthi, J. Szejtli, Reference 2(c), Chapter 3

55. (a) M. Kodaka, *J. Phys. Chem.*, **1991**, *95*, 2110

(b) M. Kodaka, *J. Am. Chem. Soc.*, **1993**, *115*, 3702

56. K. Lindner, W. Saenger, *Carbohydr. Res.*, **1982**, *99*, 103

57. J.M. Maclennan, J.J. Stezowski, *Biochem. Biophys. Res. Commun.*, **1980**, *92*, 926

58. G.L. Bertrand, J.R. Faulkner, S.M. Han, D.W. Armstrong, *J. Phys. Chem.*, **1989**, *93*, 6863

59. T.C. Bruice, S.J. Benkovic, *Bioorganic Mechanisms*, Vol. I, W.A. Benjamin, Inc., New York, **1966**

60. M.T. Behme, E.H. Cordes, *J. Org. Chem.*, **1964**, *29*, 1255

61. J.A. Shafer, H. Morawetz, *J. Org. Chem.*, **1963**, *28*, 1899

62. R. Fornasier, P. Scrimin, U. Tonellato, *Tetrahedron Lett.*, **1983**, *24*, 5541

63. R. Fornasier, F. Reniero, P. Scrimin, U. Tonellato, *J. Chem. Soc., Perkin Trans. 2*, **1987**, 193

64. Y. Ihara, E. Nakanishi, M. Nango, J. Koga, *Bull. Chem. Soc. Jpn.*, **1986**, *59*, 1901

65. G.L. Trainor, R. Breslow, *J. Am. Chem. Soc.*, **1981**, *103*, 154

66. (a) E. Sondheimer, R.W. Holley, *J. Am. Chem. Soc.*, **1954**, *76*, 2467

(b) E. Sondheimer, R.W. Holley, *J. Am. Chem. Soc.*, **1957**, *79*, 3767

67. I. Tinoco, *Adv. Chem. Phys.*, **1962**, *4*, 113

APPENDIX

The k_u values (i.e., k_{obs} at $[CD]_o = 0$) obtained for each ester in the different experiments were found to differ from each other, sometimes by as much as 10%, probably due to subtle differences in the pH of the buffers. Therefore, k_u values were measured for all the esters separately using the same buffer, k_u^{scal}, and rate constants obtained in all other experiments were scaled to these k_u^{scal} values using the equation below. Scaling affects the rate constants k_u, k_c, k_2 and k_{c2}, but does not affect the important terms K_s, k_c/k_u, K_{ts} (= k_u/k_2) and K'_{ts} (= k_c/k_{c2}). The scaled rate constants are given in the following tables.

$$k_{obs} = \frac{(k_{obs} \text{ at each } [CD]_o)(k_u^{scal})}{(k_{obs} \text{ at zero } [CD]_o)}$$

Table A.1 Data for cleavage of BOC-Esters by α-CD.[a]

k_{obs} (s^{-1})							
$[CD]_o$ (mM)	Gly	L-Ala	L-Met	L-Leu	L-Ile	L-Trp[b]	L-Phe[c]
0.0	0.746	0.447	0.560	0.267	0.0491	0.283	0.365
4.0	1.19	0.658	0.936	0.445	0.0714	0.396	0.444
8.0	1.57	0.823	1.27	0.608	0.0957	0.485	0.503
16.0	2.15	1.14	1.80	0.891	0.132	0.660	0.641
24.0	2.56	1.36	2.20	1.13	0.161	0.806	0.762
32.0	2.78	1.55	2.62	1.30	0.191	0.956	0.871
40.0	3.00	1.73	2.87	1.51	0.215	1.06	0.968

$[CD]_o$ (mM)	L-Gln	D-Gln	D-Phe[c]	β-Ala		$[CD]_o$ (mM)	L-Asn[d]
0.0	2.08	2.09	0.363	0.12		0.0	4.65
4.0	2.41	2.32	0.411	0.326		2.0	5.03
8.0	2.69	2.57	0.458	0.505		4.0	5.26
16.0	3.20	2.86	0.542[e]	0.775		8.0	5.88
24.0	3.54	3.22	0.635	0.974		12.0	6.36
32.0	3.80	3.40	0.718	1.13		16.0	6.72
40.0	4.06	3.58	0.789	1.24		20.0	6.97

[a] At 25 °C, in 0.2 M phosphate buffer, pH 11.6, containing 0.1%, [b] 5%, and [c] 10% acetonitrile. [d] In 0.2 M carbonate buffer, pH 10.6 containing 0.1% acetonitrile. [e] Point omitted from analysis.

Table A.2 Data for cleavage of CBZ-Esters by α-CD.[a]

k_{obs} (s^{-1})							
$[CD]_o$ (mM)	Gly	L-Ala	L-Val	L-Leu	L-Ile	L-Trp[b]	L-Phe[c]
0.0	1.02	0.590	0.0874	0.356	0.0599	0.437	0.509
4.0	1.66	0.993	0.183	0.762	0.126	0.566	0.565
8.0	2.10	1.46	0.315	1.20	0.202	0.676	0.618
16.0	2.59	2.35	0.544	2.13	0.392	0.916	0.717
24.0	2.79	3.30	0.765	2.93	0.559	1.15	0.820
32.0	2.91	4.07	0.950	3.96	0.706	1.35	0.960
40.0	2.93	4.85	1.14	4.79	0.822	1.55	1.06

$[CD]_o$ (mM)	L-Gln	D-Phe[c]	β-Ala	Gly-Gly		$[CD]_o$ (mM)	L-Asn[d]
0.0	2.62	0.512	0.130	4.68		0.0	5.84
4.0	3.26	0.549	0.483	8.27		2.0	6.37
8.0	3.89	0.589	0.813	11.5		4.0	6.61
16.0	5.11	0.678	1.35	17.2		8.0	7.32
24.0	6.42	0.760	1.73	22.5		12.0	7.90
32.0	7.39	0.842	2.02	26.0		16.0	8.49
40.0	8.45	0.906	2.23	30.2		20.0	8.87

[a] At 25 °C, in 0.2 M phosphate buffer, pH 11.6, containing 0.1%, [b] 5%, and [c] 10% acetonitrile.
[d] In 0.2 M carbonate buffer, pH 10.6 containing 0.1% acetonitrile.

Table A.3 Data for cleavage of BOC-Esters by β-CD.[a]

k_{obs} (s^{-1})							
$[CD]_o$ (mM)	Gly	L-Ala	L-Met	L-Leu	L-Ile	L-Trp[b]	L-Phe[c]
0.0	0.746	0.447	0.560	0.267	0.0491	0.283	0.365
1.0	2.42	-	-	-	-	-	1.96
2.0	3.26	1.98	2.33	1.08	0.365	4.25	3.05
3.0	-	-	-	-	-	-	3.89
4.0	4.14	2.68	3.11	1.38	0.608	5.09	4.6
6.0	4.86	3.25	3.74	1.63	0.832	5.85	5.72
8.0	5.62	3.66	4.27	1.84	1.02	6.50	6.99
10.0	5.97	4.12	4.8	2:06	1.23	7.11	7.89

$[CD]_o$ (mM)	L-Gln	D-Gln	D-Phe[c]	β-Ala		$[CD]_o$ (mM)	L-Asn[d]
0.0	2.08	2.09	0.363	0.120		0.0	4.65
1.0	-	-	1.89	-		0.5	3.93
2.0	4.67	2.87	2.69	1.38		1.0	3.66
3.0	-	-	3.17	-		2.0	3.45
4.0	5.83	3.24	3.55	1.85		3.0	3.42
6.0	6.79	3.53	3.91	2.14		4.0	3.43
8.0	7.63	3.78	4.23	2.38		6.0	3.46
10.0	8.05	4.01	4.36	2.54		8.0	3.60
						10.0	3.78

[a] At 25 °C, in 0.2 M phosphate buffer, pH 11.6, containing 0.1%, [b] 5%, and [c] 10% acetonitrile.
[d] In 0.2 M carbonate buffer, pH 10.6 containing 0.1% acetonitrile.

Table A.4 Data for cleavage of CBZ-Esters by β-CD.[a]

k_{obs} (s^{-1})							
$[CD]_o$ (mM)	Gly	L-Ala	L-Val	L-Leu	L-Ile	L-Trp[b]	L-Phe[c]
0.0	1.02	0.590	0.0874	0.356	0.0599	0.437	0.509
1.0	-	-	-	-	0.135	-	-
2.0	3.55	2.13	0.269	0.904	0.202	3.57	1.82
4.0	4.87	3.08	0.448	1.10	0.338	5.69	2.82
6.0	5.84	3.78	0.565	1.26	-	6.19	3.62
8.0	6.43	4.33	0.684	1.33	0.492	6.64	4.33
10.0	6.97	4.80	0.779	1.44	0.562	7.35	4.76

$[CD]_o$ (mM)	L-Gln	D-Phe[c]	β-Ala	Gly-Gly		$[CD]_o$ (mM)	L-Asn[d]
0.0	2.62	0.512	0.130	4.68		0.0	5.84
1.0	3.87	-	-	11.5		1.0	5.63
2.0	4.79	1.28	1.43	16.0		2.0	5.56
4.0	6.31	1.83	2.13	21.7		4.0	5.6
6.0	-	2.23	2.57	25.9		6.0	5.79
8.0	8.38	2.54	2.88	27.9		8.0	5.97
10.0	9.17	2.75	3.12	29.1		10.0	6.15

[a] At 25 °C, in 0.2 M phosphate buffer, pH 11.6, containing 0.1%, [b] 5%, and [c] 10% acetonitrile.
[d] In 0.2 M carbonate buffer, pH 10.6 containing 0.1% acetonitrile.

Table A.5 Data for cleavage of BOC-Esters by γ-CD.[a]

k_{obs} (s^{-1})							
$[CD]_o$ (mM)	Gly	L-Ala	L-Met	L-Leu	L-Ile	L-Trp[b]	L-Phe[c]
0.0	0.746	0.447	0.560	0.267	0.0491	0.283	0.365
1.0	1.08	0.664	0.791	0.368	0.0586	0.652	0.656
2.0	1.42	0.870	1.02	0.469	0.0675	1.06	0.925
4.0	2.02	1.24	1.41	0.653	0.0830	1.49	1.41
6.0	2.57	1.54	1.72	0.799	0.105	1.79	1.84
8.0	3.06	1.85	2.00	0.924	0.121	1.95	2.24
10.0	3.45	2.09	2.22	1.02	0.133	2.11	2.54

$[CD]_o$ (mM)	D-Phe[c]	β-Ala
0.0	0.363	0.120
1.0	0.439	0.208
2.0	0.514	0.275
4.0	0.645	0.401
6.0	0.764	0.515
8.0	0.865	0.608
10.0	0.966	0.694

$[CD]_o$ (mM)	L-Gln	D-Gln	L-Asn[d]
0.0	2.08	2.09	4.65
2.0	2.74	2.26	4.80
4.0	3.44	2.40	4.91
8.0	4.62	2.67	5.06
12.0	5.62	2.89	5.24
16.0	6.65	3.13	5.26
20.0	7.25	3.33	5.37

[a] At 25 °C, in 0.2 M phosphate buffer, pH 11.6, containing 0.1%, [b] 5%, and [c] 10% acetonitrile.
[d] In 0.2 M carbonate buffer, pH 10.6 containing 0.1% acetonitrile.

Table A.6 Data for cleavage of CBZ-Esters by γ-CD.[a]

k_{obs} (s^{-1})							
$[CD]_o$ (mM)	Gly	L-Ala	L-Val	L-Leu	L-Ile	L-Trp[b]	L-Phe[c]
0.0	1.02	0.590	0.0874	0.356	0.0599	0.437	0.509
1.0	3.53	3.66	0.226	1.96	0.133	1.38	1.63
2.0	5.55	5.94	0.326	3.03	0.192	2.16	2.70
4.0	8.48	8.84	0.474	4.47	0.272	3.14	4.30
6.0	10.7	10.7	0.558	5.56	0.332	3.65	5.36
8.0	12.1	11.8	0.614	6.02	0.355	4.25	6.34
10.0	12.8	12.4	0.661	6.46	0.391	4.70	6.90

$[CD]_o$ (mM)	L-Gln	D-Phe[c]	β-Ala	$[CD]_o$ (mM)	Gly-Gly	$[CD]_o$ (mM)	L-Asn[d]
0.0	2.62	0.512	0.130	0.0	4.68	0.0	5.84
1.0	6.25	0.729	1.73	2.0	19.4	2.0	6.59
2.0	9.05	0.960	2.71	4.0	26.3	4.0	6.90
4.0	12.5	1.25	3.81	8.0	30.4	8.0	7.24
6.0	15.2	1.53	4.31	16.0	27.3	12.0	7.58
8.0	16.3	1.79	4.73	24.0	22.9	16.0	7.60
10.0	17.6	1.92	4.82	32.0	19.5	20.0	7.66
				40.0	17.1		

[a] At 25 °C, in 0.2 M phosphate buffer, pH 11.6, containing 0.1%, [b] 5%, and [c] 10% acetonitrile.
[d] In 0.2 M carbonate buffer, pH 10.6 containing 0.1% acetonitrile.

Table A.7 Data for cleavage of N-Hydroxysuccinimide Esters of BOC-Pro enantiomers by CDs.[a]

k_{obs} (s^{-1})								
$[\alpha\text{-CD}]_o$ (mM)	L-Pro	D-Pro	$[\beta\text{-CD}]_o$ (mM)	L-Pro	D-Pro	$[\gamma\text{-CD}]_o$ (mM)	L-Pro	D-Pro
0.0	1.56	1.56	0.0	1.56	1.56	0.0	1.56	1.56
1.0	1.73	1.71	2.0	48.3	12.8	1.0	3.01	2.44
2.0	1.88	1.87	3.0	54.0	14.3	2.0	4.49	3.23
4.0	2.17	2.27	4.0	55.5	16.3	4.0	6.51	4.76
6.0	2.58	2.61	6.0	58.6	17.0	6.0	8.18	5.84
8.0	2.85	2.90	8.0	59.3	17.6	8.0	9.62	6.69
10.0	3.17	3.09	10.0	60.1	17.7	10.0	10.9	7.56

[a] At 25 °C, in 0.2 M phosphate buffer, pH 11.6, containing 0.1%.